PHILOSOPHICAL TRANSACTIONS OF THE ROYAL SOCIETY A
MATHEMATICAL, PHYSICAL & ENGINEERING SCIENCES

A Review of Geophysical Constraints on the Deep Structure of the Tibetan Plateau, the Himalaya and the Karakoram, and their Tectonic Implications

P. Molnar

Phil. Trans. R. Soc. Lond. A 1988 **326**, 33-88
doi: 10.1098/rsta.1988.0080

Phil. Trans. R. Soc. Lond. A **326**, 33–88 (1988) [33]
Printed in Great Britain

A review of geophysical constraints on the deep structure of the Tibetan Plateau, the Himalaya and the Karakoram, and their tectonic implications

By P. Molnar†

Laboratoire de Géophysique Interne et Tectonophysique (*CNRS U.A.* 733), *Institut de Recherches Interdisciplinaires de Géologie et Mécanique*, *B.P.* 68, *Université Scientifique*, *Technique*, *et Médicale de Grenoble*, 38402 *Saint Martin d'Hères Cèdex*, *France*

The Tibetan Plateau, the Himalaya and the Karakoram are the most spectacular consequences of the collision of the Indian subcontinent with the rest of Eurasia in Cainozoic time. Accordingly, the deep structures beneath them provide constraints on both the tectonic history of the region and on the dynamic processes that have created these structures.

The dispersion of seismic surface waves requires that the crust beneath Tibet be thick: nowhere less than 50 km, at least 65 km, in most areas, but less than 80 km in all areas that have been studied. Wide-angle reflections of P-waves from explosive sources in southern Tibet corroborate the existence of a thick crust but also imply the existence of marked lateral variations in that thickness, or in the velocity structure of the crust. Thus isostatic compensation occurs largely by an Airy-type mechanism, unlike that, for instance, of the Basin and Range Province of western North America where a hot upper mantle buoys up a thin crust.

The P-wave and S-wave velocities in the uppermost mantle of most of Tibet are relatively high and typical of those of Precambrian shields and stable platforms: $V_p = 8.1\ \mathrm{km\,s^{-1}}$ or higher, and $V_s \approx 4.7\ \mathrm{km\,s^{-1}}$. Travel times and waveforms of S-waves passing through the uppermost mantle of much of Tibet, however, require a much lower average velocity in the uppermost mantle than that of the Indian, or other, shields. They indicate a thick low-velocity zone in the upper mantle beneath Tibet, reminiscent of tectonically active regions. These data rule out a shield structure beneath northern Tibet and suggest that if such a structure does underlie part of the plateau, it does so only beneath the southern part.

Lateral variations in the upper-mantle structure of Tibet are apparent from differences in travel times of S-waves from earthquakes in different parts of Tibet, in the attenuation of short-period phases, Pn and Sn, that propagate through the uppermost mantle of Tibet, and in surface-wave dispersion for different paths. The notably lower velocities and the greater attenuation in the mantle of north–central Tibet than elsewhere imply higher temperatures there and are consistent with the occurrence of active and young volcanism in roughly the same area. Surface-wave dispersion across north–central Tibet also requires a thinner crust in that area than in most of the plateau. Consequently the relatively uniform height of the plateau implies that isostatic compensation in the north–central part of Tibet occurs partly because the density of the relatively hot material in the upper mantle is lower than that elsewhere beneath Tibet, the mechanism envisioned by Pratt.

Several seismological studies provide evidence consistent with a continuity of the Indian Shield, and its cold thick lithosphere, beneath the Himalaya. Fault-plane solutions and focal depths of the majority of moderate earthquakes in the Himalaya

† Permanent address: Department of Earth, Atmospheric, and Planetary Sciences, Massachusetts Institute of Technology, Cambridge, Massachusetts 02139, U.S.A.

are consistent with their occurring on the top surface of the gently flexed, intact Indian plate that has underthrust the Lesser Himalaya roughly 80–100 km or more. P-waves from explosions in southern Tibet and recorded in Nepal can be interpreted as wide-angle reflections from this fault zone. P-wave delays across the Tarbela network in Pakistan from distant earthquakes indicate a gentle dip of the Moho beneath the array without pronounced later variations in upper-mantle structure. High Pn and Sn velocities beneath the Himalaya and normal to early S-wave arrival times from Himalayan earthquakes recorded at teleseismic distances are consistent with Himalaya being underlain by the same structure that underlies India.

Results from explosion seismology indicate an increase in crustal thickness from the Indo–Gangetic Plain across the Himalaya to southern Tibet, but Hirn, Lépine, Sapin and their co-workers inferred that the depth of the Moho does not increase smoothly northward, as it would if the Indian Shield had been underthrust coherently beneath the Himalaya. They interpreted wide-angle reflections as evidence for steps in the Moho displaced from one another on southward-dipping faults. Although I cannot disprove this interpretation, I think that one can recognize a sequence of signals on their wide-angle reflection profiles that could be wide-angle reflections from a northward-dipping Moho.

Gravity anomalies across the Himalaya show that both the Indo–Gangetic Plain and the Himalaya are not in local isostatic equilibrium. A mass deficit beneath the plain is apparently caused by the flexure of the Indian Shield and by the low density of the sedimentary rock in the basin formed by the flexure. The mass excess in the Himalaya seems to be partly supported by the strength of the Indian plate, for which the flexural rigidity is particularly large.

An increase in the Bouguer gravity gradient from about 1 mGal km^{-1} (1 mGal = 10^{-3} cm s^{-2}) over the Indo–Gangetic Plain to 2 mGal km^{-1} over the Himalaya implies a marked steepening of the Moho, and therefore a greater flexure of the Indian plate, beneath the Himalaya. This implies a northward decrease in the flexural rigidity of the part of the Indian plate underlying the range. Nevertheless, calculations of deflections of elastic plates with different flexural rigidities and flexed by the weight of the Himalaya show larger deflections and yield more negative gravity anomalies than are observed. Thus, some other force, besides the flexural strength of the plate, must contribute to the support of the range. A bending moment applied to the end of the Indian plate could flex the plate up beneath the range and provide the needed support. The source of this moment might be gravity acting on the mantle portion of the subducting Indian continental lithosphere with much or all of the crust detached from it.

Seismological studies of the Karakoram are consistent with its being underlain by particularly cold material in the upper mantle. Intermediate-depth earthquakes occur between depths of 70 and 100 km but apparently do not define a zone of subducted oceanic lithosphere. Rayleigh-wave phase velocities are particularly high for paths across this area and imply high shear wave velocities in the upper mantle. Isostatic gravity anomalies indicate a marked low of 70 mGal over the Karakoram, which could result from a slightly thickened crust pulled down by the sinking of cold material beneath it.

Geophysical constraints on the structure of Tibet, the Himalaya and the Karakoram are consistent with a dynamic uppermost mantle that includes first, the plunging of cold material into the asthenosphere beneath southern Tibet and the Karakoram, as the Indian plate slides beneath the Himalaya, and second, an upwelling of hot material beneath north–central Tibet. The structure is too poorly resolved to require such dynamic flow, but the existence for both a hot uppermost mantle beneath north–central Tibet and a relatively cold uppermost mantle beneath southern Tibet and the Karakoram seem to be required.

PHILOSOPHICAL TRANSACTIONS OF THE ROYAL SOCIETY A MATHEMATICAL, PHYSICAL & ENGINEERING SCIENCES

Introduction

The deep structure of the Himalaya and Tibet is poorly known, compared with that of much of the world, but by the same comparison, its geophysical study has a tradition of importance exceeded by few areas. The concept of isostasy (Airy 1855), which perhaps represents the birth of geophysics as a subdiscipline of and a contributor to the geological sciences, grew from geodetic work in India and from the realization that the deep structure of the Himalaya and Tibet had contributed to large discrepancies in surveyed positions (Pratt 1855). With the invention of gravity meters, the Himalaya became an important testing ground for theories of isostasy, and deviations from local isostatic equilibrium as large as those of the Himalaya are found in only a few other regions of the Earth. Now in the 1980s, with a generation of Earth scientists educated on the premises that geophysics can be used to solve geological problems, that plate tectonics is a fact, and that dynamic processes controlling the tectonic evolution of the Earth are driven largely by gravity acting on density differences within the Earth, the Himalaya and Tibet once again are testing grounds for theories of orogenesis. Accordingly, considerable progress in defining the deep structure of the Himalaya and Tibet has been made on the last 10 years, and a review at this time seems appropriate given both the likelihood that little new information will be gathered in the next few years and the result that most existing data have been analysed with modern techniques.

The physiographic scale of the Himalaya and Tibet make them unusually prominent features on the Earth (figures 1 and 2), and as such an understanding of the processes that created them is likely to carry with it the understanding of how many smaller mountain belts

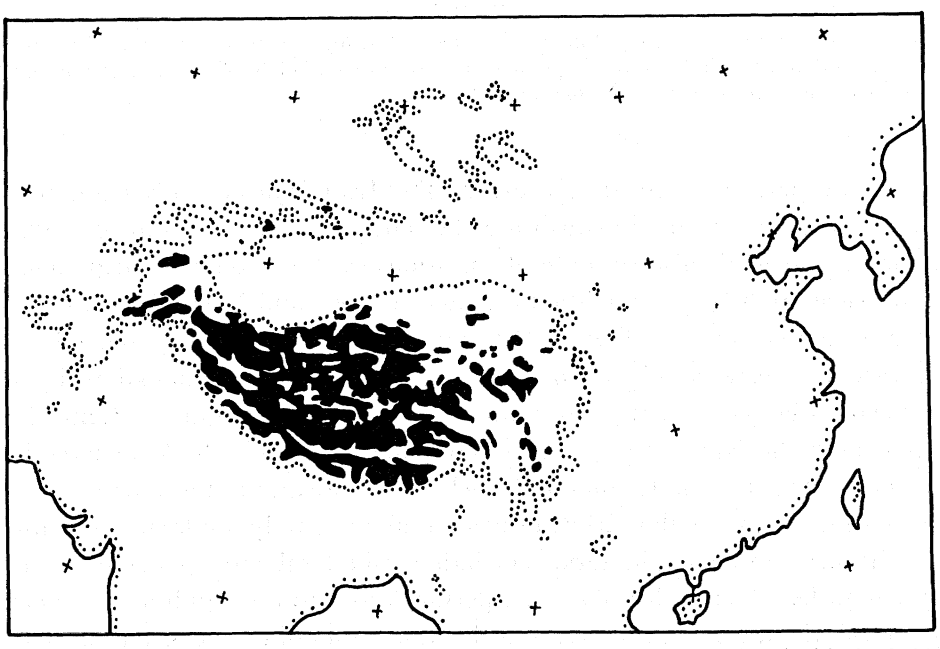

Figure 1. Simple contour map of part of Asia, with areas higher than 5000 m shaded and with the 2500 m contour dotted (drawn from Cauët *et al.* 1957, pp. 34–35). The Tibetan Plateau comprises the area that is mostly higher than 5000 m. A similar map for any other continent would be nearly entirely white, with only specks of black here and there. No part of Europe or Australia lies above 5000 m. The Himalaya follows the southern margin of Tibet, and the Karakoram constitute the large area higher than 5000 m in the northwest corner of Tibet (see figure 4).

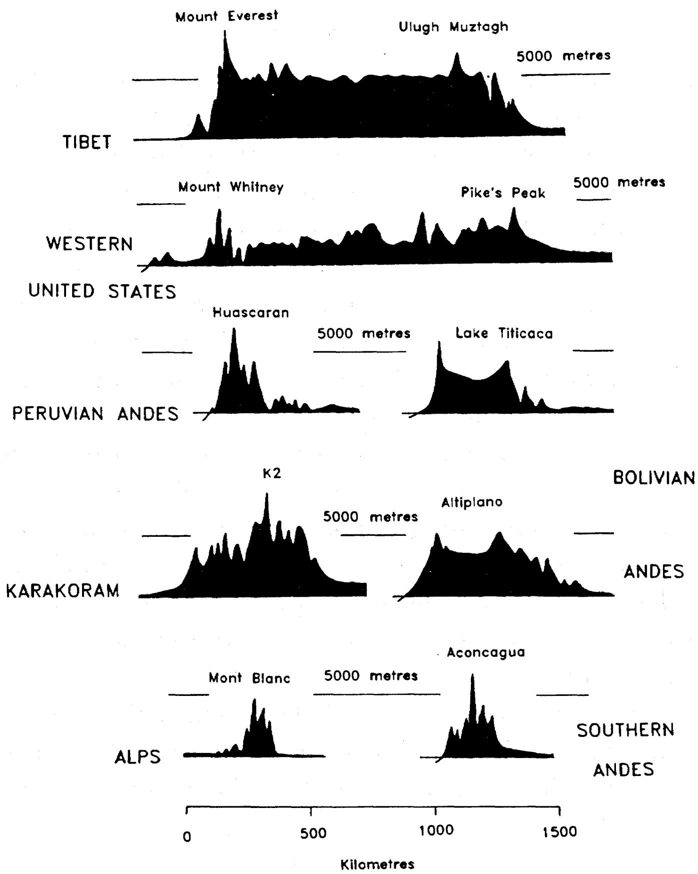

FIGURE 2. Profiles of elevation across selected mountain ranges, showing the much greater height and extent of the Tibetan Plateau than other intermountain plateaux and the greater height of the Karakoram than most other ranges (drawn from maps in the *Times Atlas of the World*).

and intermontane plateaux formed or evolved. The Himalaya not only contain the highest peaks on the Earth, but probably constitute the longest active mountain belt that shares a relatively common geologic history. Lateral variations exist, but they are negligible compared with the differences among the individual ranges of Europe and North Africa, which together form a chain of comparable length with that of the Himalaya. Similarly, the Tibetan Plateau is not only very obviously the highest plateau on Earth, but its lateral extent, by almost any definition, makes it larger than any other intermontane plateau (figure 2). Thus the dynamic processes that built the Himalaya and Tibet are likely to include the less energetic processes that have constructed the smaller mountain belts and plateaux of the Earth.

In simple terms, the engine that drives orogenesis almost surely resides in the mantle and not in the crust. Its measurable manifestations include both lateral heterogeneities in the structure of the upper mantle, which reflect dynamic perturbations to the equilibrium associated with a radially symmetric, layered structure, and the kinematics of the deformation that results in the structures visible at the surface of the Earth. Although geophysical methods have contributed to an increased knowledge of the kinematics of deformation, they are virtually the only methods capable of resolving the deep structure of orogenic belts.

This review focuses on the structure of the upper mantle and on its boundary with the overlying crust, for it is in this depth range that the dynamic processes affecting orogenesis are most likely to reveal themselves in the internal structure of the Earth. Among the many subdisciplines of geophysics, the two that contribute most of the constraints on lateral variations in the deep structure are gravity and seismology. Variations in the Earth's gravity field are caused by heterogeneities in the distribution of mass, and therefore density, in the Earth. The analysis of variations in the gravity field, or of gravity anomalies, can be a very expedient method for proving that a particular hypothetical structure (or model) is wrong. Because of their inherent non-uniqueness, however, only when constrained by simplifying assumptions can gravity anomalies demonstrate that a particular structure is required. Variations in seismic wave velocities in the Earth, in general, can be resolved with much greater precision than those of density, and accordingly most of what we know of the deep interior and its lateral variations derives from studies of seismic waves. The present review concentrates on these two sources of information.

Because both the geologic evolution and the deep structure of the Himalaya and of the Karakoram differ from those of Tibet, I consider these three areas separately. This is facilitated by the relative importances of the two types of data in these areas.

This review begins with Tibet, briefly noting the constraints of the one published gravity datum from its interior and allusions to unpublished gravity data, followed by a summary of results from explosion seismology, from seismic surface waves, and from regionally and teleseismically recorded body waves. Seismic studies with explosive sources yield weak constraints on the deep structure of the interior of Tibet, but tight constraints for the area south of the Indus–Tsangpo Suture Zone. It is important to realize that most geologists not concerned with Quaternary tectonics place the boundary of the Himalaya at this suture, but the Quaternary and active tectonics of the area between the suture and the Greater Himalaya is similar to that of Tibet and very different from that of the Himalaya farther south (Molnar & Tapponnier 1978). Similarly the deep structure of this area suggests a continuity with Tibet. Accordingly, I include the area north of the Greater Himalaya within the Tibetan Plateau.

Seismic experiments in the Himalaya yield data that either are ambiguous or yield surprising results, depending upon one's point of view. Although Hirn *et al.* (1984*a–c*; Hirn & Sapin 1984; Lépine *et al.* 1984; Sapin *et al.* 1985) have stressed the differences in what these data suggest from what has been inferred from gravity anomalies in the Himalaya, I focus this review more on the gravity anomalies than on the seismic data. Finally, I consider tentative implications of gravity anomalies and aspects of seismology for the structure of Tibet's western and northwestern margins, across the Karakoram and western Kunlun belts, which may offer a key to understanding the dynamics of the continuing collision and the penetration of India into the rest of Asia.

Deep structure of the Tibetan Plateau

Introduction

Beginning with Argand (1924), and perhaps before his work, the supposition that the high elevation of the Tibetan Plateau is compensated by a thick crust has underlain virtually all ideas concerning the geologic evolution of the plateau. There now seems little doubt that the crust of the Tibetan Plateau is thick: the thickness is at least 50 km everywhere and closer to 65–70 km in most of the plateau. At the same time the evidence that demonstrates the existence of thick crust, while convincing, is not simple and has required approaches that are somewhat different from those used elsewhere. In my opinion, the proof that the crust is thicker than 55 km throughout most of the plateau was obtained only in 1979 by Wang-ping Chen.

Argand (1924) envisioned the crustal thickening to have occurred by the underthrusting of the Indian subcontinent beneath the entire plateau (figure 3). This idea has received support

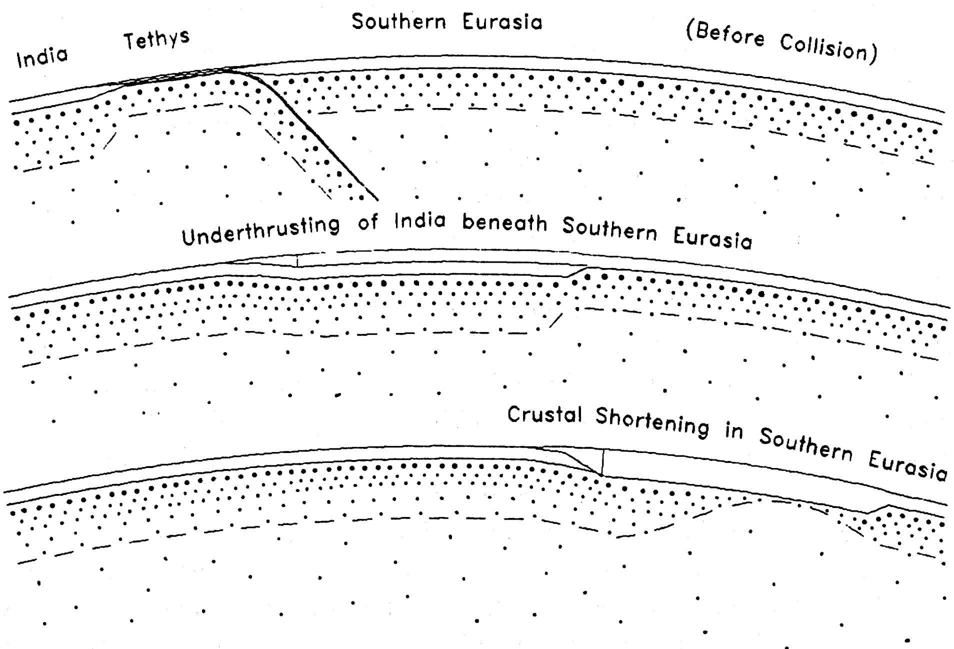

FIGURE 3. Simple cross sections illustrating basic ideas for how the Tibetan Plateau formed. Top cross section shows oceanic lithosphere, carrying India, being subducted beneath southern Eurasia before the collision of India with Eurasia. No attempt has been made to illustrate possible heterogeneities in the Asian lithosphere before the collision. Middle cross section illustrates Argand's (1924) concept of the Indian subcontinent underthrusting southern Eurasia, with the corollary that the entire Indian lithosphere has been underthrust (Barazangi & Ni 1982; Ni & Barazangi 1983, 1984; Powell & Conaghan 1973, 1975; Seeber *et al.* 1981). No attempt has been made to distinguish variations on this idea such as that of Zhao & Morgan (1985). The bottom cross section indicates an evolution of Tibet in which the crust of southern Asia has shortened in its north–south dimension (Dewey & Burke 1983; England & Houseman 1986) as India has penetrated into Eurasia. The evolution of the lithosphere beneath southern Eurasia is drawn as if it has undergone convective response to the thickening of it (see figure 22 for more discussion).

from extrapolations of geologic cross sections in the Himalaya (Klootwijk *et al.* 1985; Powell & Conaghan 1973, 1975), from extrapolations of seismological constraints on the orientations of active faults at the Himalaya (Ni & Barazangi 1984; Seeber & Armbruster 1981; Seeber *et al.* 1981), from the areal extent of the plateau compared with the areal extent of material presumed to have lain northeast of India and west of Australia before the dispersal of Gondwana (Curray & Moore 1974; Johnson *et al.* 1976), and finally from some seismological studies of Tibet itself (Barazangi & Ni 1982; Ni & Barazangi 1983). Given the convictions of so many other Earth scientists that India has not underthrust the whole of Tibet, however, it is clear that none of the evidence presented in support of this concept has been overwhelmingly convincing.

Seismic studies of the lower crust and upper mantle of Tibet inherently lack the information needed to decide how the structure has evolved, but such studies can be used to ask whether or not the structure that presently underlies Tibet is similar to that presently underlying India. Because much of the Indian subcontinent consists of a Precambrian shield, for which the upper-mantle structure is, in general, very distinctive, seismological studies can resolve whether Tibet is at present underlain by a shield, and the answer to this question is clearly no (Lyon-Caen 1986). This does not, however, prove that Tibet was not underthrust by a shield at some earlier date and that subsequently the structure changed.

Finally, seismological studies are now capable of resolving lateral variations in crustal and upper-mantle structure of Tibet, and despite the remarkably uniform height of the plateau, surprisingly large variations in upper-mantle shear-wave velocity have been found (see, for example, Brandon & Romanowicz 1986; Molnar & Chen 1984), and they, in turn, imply large variations in temperature beneath the plateau.

This review addresses the evidence concerning these three aspects of Tibet's structure: the thickness of the crust beneath the plateau, the average velocity structure in its upper mantle, and lateral variations in the structure of the crust and upper mantle.

The crustal thickness of the Tibetan Plateau

Gravity anomalies

To my knowledge there is only one published gravity measurement from the interior of the Tibetan Plateau, made by Amboldt (1948) in the 1920s with a pendulum gravity meter. The free-air anomaly of 18 mGal† implies a state of nearly isostatic equilibrium, but clearly alone it places no constraint on the mechanism of isostatic compensation.

Profiles of gravity anomalies along the main road in eastern Tibet, from the Himalaya through Lhasa to Golmud and north of the plateau (figure 4) are apparently characterized by the large negative Bouguer anomalies (−500 mGal) that must exist for isostatic equilibrium to exist, and if an Airy-type mechanism prevails (Tang *et al.* 1981; Teng 1981; Teng *et al.* 1980; Wang *et al.* 1982; Zhou *et al.* 1981). Variations of gravity over distances of 50–200 km along the profiles are shown to be small, at most only 30 mGal. The largest such variation lies near the Indus–Tsangpo Suture (figure 4) and corresponds to a 30 mGal low (Tang *et al.* 1981; Zhou *et al.* 1981). Given the lack of information describing how these plots were obtained, however, one cannot know if such a low is defined by more than one measurement or if it is a consequence of how the data were projected onto the profile, for instance from an area farther west where altitudes are higher. In my opinion, the absence of raw data and a published discussion of them makes it risky to conclude more than that deviations from isostatic equilibrium are not enormous.

Explosion seismology in Tibet

Seismic refraction. Profiles have been shot in Tibet both by Chinese scientists from the Academy of Sciences (Institute of Geophysics, Academy of Sciences 1981; Teng *et al.* 1980, 1981, 1983) and jointly by French and Chinese scientists, in this case mostly from the Ministry of Geology (Hirn *et al.* 1984*a–c*; Sapin *et al.* 1985; Teng *et al.* 1985).

In 1976 and 1977, Chinese scientists carried out a seismic refraction program along a profile from the Great Himalaya into southern Tibet, essentially along the road from the border of Sikkim, India to the lake Nam Tso (figure 4). The total length is about 450 km. Teng *et al.* (1980, 1981, 1983; Institute of Geophysics, Academy of Sciences 1981) inferred a thick crust

† 1 mGal = 10^{-3} cm s^{-2}.

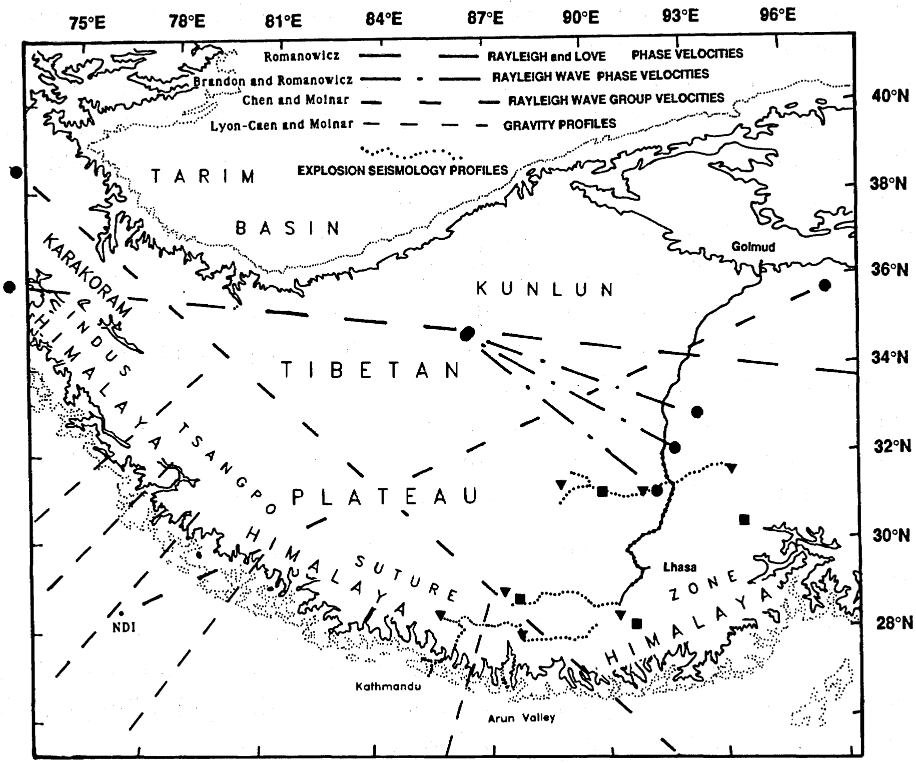

FIGURE 4. Map of the Tibetan Plateau, the Himalaya and the Karakoram, showing locations of seismic refraction and wide-angle reflection profiles and shotpoints (inverted triangles), relevant paths for measured surface-wave dispersion with black circles showing epicentres of earthquakes used, temporary long-period seismograph stations (squares) (Jobert *et al.* 1985), gravity profiles, and the road from Lhasa to Golmud. Contours for 1500 m (dotted) and 3000 m (solid line) outline the plateau.

of 70–73 km beneath Tibet and decreasing beneath the Himalaya. They reported a structure with five layers, including a pronounced low-velocity zone, overlying a mantle with a P-wave velocity of 7.95 km s^{-1} in one area, of 8.4 km s^{-1} in another, and with an average of 8.15 ± 0.03 km s^{-1}. Beneath the Himalaya, the interfaces of these layers are shown to dip toward the north, with slightly different velocities from those further north (Teng *et al.* 1981, 1983).

Although Teng *et al.* (1981, 1983; Institute of Geophysics, Academy of Sciences 1981) show some particularly clear seismograms and plots of observed and calculated travel time curves, I found the discussion of the data too brief for me to be able to evaluate the conclusions. In particular, I am unable to recognize clear signals that might be Pn phases on the plot showing seismograms recorded at distances greater than 250 km (figure 3 of Institute of Geophysics, Academy of Sciences 1981; reproduced as figure 4 of Teng *et al.* 1981). The other well-illustrated profiles (figure 2 of Institute of Geophysics, Academy of Sciences, 1981; or figure 3 of Teng *et al.* 1981, 1983) show clear signals but only from distances smaller than 250 km, for which refractions from the Moho would not be the first arrivals.

The joint Chinese and French studies represent well-planned experiments designed to elucidate the deep crustal structure and, in particular, the shape of the Moho, but in my opinion too little space was devoted either to showing or to discussing the seismograms. Moreover, following long traditions in the presentation of seismic refraction results, some traces are obscured by dark black lines that show interpretations, and in the shorter of the papers discussing the results, only one interpretation that fits the data is shown, making an evaluation of the non-uniqueness or the uncertainties difficult. As a result, my review of their results is clouded by an inability to decide which aspects of their inferences are required, as well as by prejudices that makes me dubious of some of them.

These studies fall into two types: reversed refraction profiles with stations spaced at different distances between the two shot points at the ends of the profile, and profiles recorded at roughly constant distances from sources (fan-profiles), designed to record strong wide-angle reflections from interfaces with abrupt velocity contrasts, such as the Moho. Of the two refraction profiles, one was 300 km north of the Indus–Tsangpo Suture Zone, and the other about 80 km south of it (figure 4).

The profile shot parallel to and south of the Indus–Tsangpo Suture Zone yields the better constrained deep structure (Hirn *et al.* 1984*a*, *c*). Seismographs were distributed over a distance of 500 km, 60–100 km south of the suture zone, approximately halfway between the high peaks of the Greater Himalaya and the suture zone (see also Teng *et al.* 1985). Explosives were detonated at both ends and approximately in the middle of the line, and correlatable signals were recorded at distances greater than 400 km. In addition, one of the shots was recorded along the suture zone at distances of 170–270 km from the eastern shot point.

Teng *et al.* (1985) used travel times from these explosions to infer flat-layered velocity structures along four segments of the profile. Their inferred structures include from five to eight layers overlying a halfspace (mantle) with a velocity of 8.1 or 8.2 km s^{-1}. A low-velocity zone (6.0 or 6.1 km s^{-1}) is reported at the base of the crust just above the Moho. On two segments, a second low-velocity zone is shown in the upper crust. The existence of marked velocity contrasts is implied by the strong, apparently reflected, signals that define travel time curves with decreasing apparent velocity with increasing distance. The clearest is that from the Moho and was analysed in detail by Hirn *et al.* (1984*c*). Refracted signals, however, are less clear, and the reported velocities of 8.1 and 8.2 km s^{-1} for the mantle are very different from the velocity inferred from the same data by Hirn *et al.* (1984*c*), discussed below. Thus it is difficult for me to know which aspects of these multilayered structures are required.

Hirn *et al.* (1984*c*) abstained from deducing, or at least reporting, a layered velocity structure, and instead they focused attention on the strong signals at distances of 200–300 km attributed to reflections from the Moho. The arrival times at these distances imply a thick crust (thickness about 75 km), but the strength of the signals at such long distances together with the arrival times cannot be matched by an abrupt increase in velocity at the Moho, as would be required by the low-velocity zone inferred by Teng *et al.* (1985). With a series of calculations, they showed how an increase in the thickness of a transition zone between crust and mantle affects both the distance at which strong wide-angle reflections are recorded and the times when these reflected phases arrive (figure 4 of Hirn *et al.* 1984*c*).

Seismograms recorded along the suture zone from the eastern shot also show clear sharp signals at the six stations between 230 and 260 km from that shot (figure 6 of Hirn *et al.* 1984*c*). The travel times of these signals imply that the depth to the reflector is similar to that observed along the more continuous profile farther south, but the relative differences in arrival times at neighbouring receivers are sufficiently large that the lateral variations in crustal structure must exist. In any case, the depth of the Moho of about 75 km beneath the southern edge of the Tibetan Plateau, between the Greater Himalaya and the Indus–Tsangpo Suture Zone, seems to be well established.

Before reviewing Hirn's and his colleagues' constraints on the variations in the depth of the

Moho, two other results derived from their profiles just south of the suture are worth noting: one concerning the lower crust and the other the upper mantle.

First, to fit both the amplitudes of the reflections from the Moho and another set of signals, which they attribute to reflections within the crust, Hirn & Sapin (1984) suggested that attenuation in the lower crust is very high. The relative amplitudes of the signals could be matched if there were a very large difference in velocity across the intracrustal reflector, but the smaller amplitudes and the lower predominant frequencies of the more deeply reflected phases concurs with the alternative suggestion that Q in the lower crust is very low (about 100), and therefore attenuation is very high. A unique explanation for such a low Q cannot be given, but one obvious explanation is that temperature in the lower crust is high. This possibility is consistent with, but also not required by, the high heat flow measured in lakes at the eastern end of the profile (Francheteau *et al.* 1984; Jaupart *et al.* 1985). It is not obviously in accord with magnetotelluric studies, which indicate shallow but not deep layers of low electrical conductivity, and which therefore suggest high temperature at shallow depth (Pham *et al.* 1986).

Second, Hirn *et al.* (1984*c*) recorded weak, but discernable, signals from 300 km to more than 400 km from the eastern shot point, and they pointed out that these signals seem to define refractions from the Moho. They stated that signals from the western shot point are less clear, but that 'clear onsets at 300 km, 340 km, and 400 km correspond within 0.1 s' with the travel-time curve for the eastern shot point. The velocity defined by this travel-time curve is unusually high, 8.7 km s^{-1}. They noted that only a very unusually low (unreasonably low) temperature could explain such a velocity, but that 8.7 km s^{-1} is not unreasonable if anisotropy exists.

Sapin *et al.* (1985) described a profile 500 km in length within the interior of the Tibetan Plateau (figure 4). Explosives were detonated at the two ends and at a site 200 km from the western shotpoint. The major part of the discussion of Sapin *et al.* (1985) concerns the crustal structure, shallower than about 30 km, for which recordings at distances less than 200 km place strong constraints. The absence of clear arrivals refracted at the Moho do not allow a constraint to be placed on the velocity in the mantle. Clear wide-angle reflections, presumably from the Moho, were recorded from the eastern shot point, at distances greater than 200 km, but those from the western shotpoint are less clear. Such signals were recorded clearly at some recording sites, but not at neighbouring sites 10–20 km away. Sapin *et al.* (1985) noted the following cautious conclusion. 'The relevant observation is that reflections from 70 km depth from a crust–mantle boundary exist in places but the continuity and the geometry of the Moho along the...line cannot be assessed.' Thus, what is the best-documented seismic refraction study of Tibet north of the Indus–Tsangpo Suture places no constraint on the P-wave velocity in the mantle and yields only a weak evidence for the crustal thickness of about 70 km.

Wide-angle reflection profiles. Among the data presented by Hirn and his collaborators, the fan profiles, designed to record wide-angle reflections from the Moho, provide the most tantalizing information and therefore, perhaps the most difficult to interpret. Their studies of wide-angle reflections can be conveniently grouped into three sets: one beneath the Himalaya (that I defer to the discussion of the Himalaya below): a second, beneath the area just south of the Indus–Tsangpo Suture Zone: and a third, north of the suture.

Wide-angle reflections from the Moho are particularly strong from an area near the suture, where the Moho is marked by a thick transition zone, thicker than 6 km and of the order of 12 km (Hirn *et al.* 1984*c*). Whereas the wide-angle reflections imply a crustal thickness of about

75 km along the main reversed refraction profile, signals also recorded at distances of about 200 km from the eastern shotpoint but at locations south of this profile show earlier arrival times. Hirn *et al.* (1984*c*) inferred that the crustal thickness decreases to about 70 km, approximately 15 km south of the main refraction profile, suggesting the possibility of a relatively steep northward dip of the Moho of about 25° (figure 5). Reflections recorded north

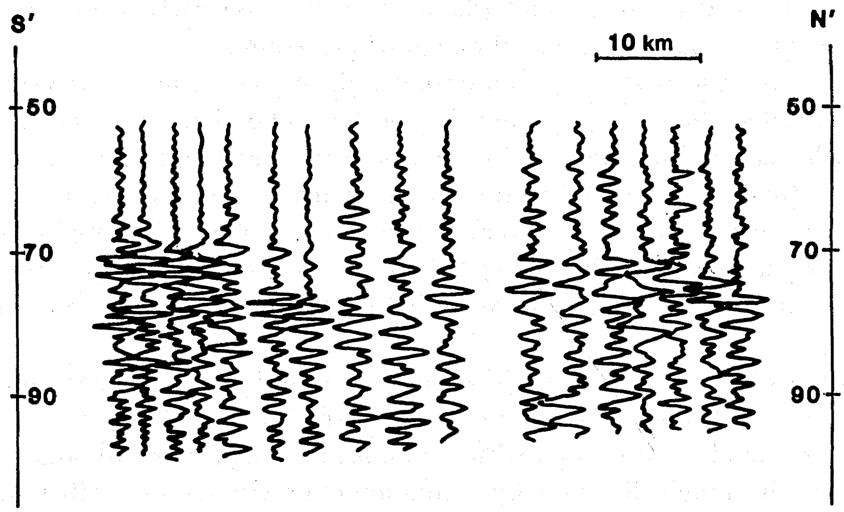

FIGURE 5. Seismograms recorded on a north–south profile roughly equidistant and 200 km west of the eastern shotpoint of the east–west profile between the Indus–Tsangpo Suture and the Greater Himalaya (figure 4). The timescale has been converted into a depth scale after correcting for different distances. The prominent phases mark strong wide-angle reflections from the Moho and indicate depths of it of 70–75 km. (From Hirn & Sapin 1984.)

of this profile show a scatter in onset times consistent with a crustal thickness between 70 and 75 km, assuming the same velocity structure of the crust as that deduced from the long refraction profile through this area (Hirn *et al.* 1984*c*). A similar fan-profile made from the shot point in the middle of this profile and recorded on a north–south line at the west end of the profile reveals sharp onsets on seven seismograms at the times corresponding to a Moho at 70 km (figure 15, discussed in more detail below). These reflection points lie between 30 and 50 km north of the crest of the High Himalaya Range but south of the main refraction line. Thus wide-angle reflections at various localities between the suture and the High Himalaya indicate a mean depth of the Moho transition zone of about 70–75 km, either with definite, if small (5 km), variations in depth, or with heterogeneity in the crustal velocity structure that translates into apparent variations in depth.

Using two shot points roughly 250 km west of the main north–south road in eastern Tibet, Hirn *et al.* (1984*b*; Allègre *et al.* 1984) made fan profiles designed to record wide-angle reflections from the Moho beneath southern Tibet. Reflections from the southern shot recorded near the suture imply that the Moho beneath the suture zone also lies about 70 km below the surface (Hirn *et al.* 1984*b*).

The recordings of wide-angle reflections farther north of the suture provide evidence for why neither the Moho nor the uppermost mantle could be studied well on the long refraction profile of Sapin *et al.* (1985) across central Tibet. The great variety in recordings requires marked variations in the structure west of the main road (figure 2 of Hirn *et al.* 1984*b*). Along some parts of the profile, strong signals arrive at the times expected for reflections from a Moho at a depth of 70 km, but at others no clear signal can be seen at these times. In some portions, clear signals are recorded at times suggesting that they represent phases reflected at depths of only 50 km, and sharp signals recorded at progressively different times on neighbouring profiles can be most simply interpreted as reflections from dipping interfaces. Thus given the complexity of the crustal structure revealed by these profiles, the failure to record continuous reflections along the 500 km long profile (Sapin *et al.* 1985) is clearly neither exceptional nor likely to be caused by poor experimental design or procedure.

Hirn *et al.* (1984*b*; Allègre *et al.* 1984) interpreted the variations in the arrival times of these clear signals as being caused by steps and dips of the Moho along the profile. Because they recognized such steps and northward dips near both the Indus–Tsangpo and the Bangong–Nujiang Suture Zones, they interpreted the variations in arrival times in terms of slip on thrust faults that penetrate into the mantle and along which the Moho in the hanging wall has been elevated with respect to that of the foot wall. This interpretation is certainly reasonable, and I do not know of data that refute it. Nevertheless, I also think that there are reasons to doubt it.

First, differences in the depth of the Moho of 20 km are inferred to persist for distances of 100 km. Even with a density contrast of only 400 kg m^{-3} at the Moho, such a difference in crustal thickness should be associated with variations in Bouguer gravity anomalies of more than 150 mGal. Given both the limited presentation of gravity data for Tibet and that those measurements were made roughly 125 km east of where the steps in the Moho have been inferred to lie, the published plots of gravity anomalies (Tang *et al.* 1981; Teng *et al.* 1980; Wang *et al.* 1982; Zhou *et al.* 1981) certainly do not disprove the inferred steps in the Moho of Hirn *et al.* (1984*b*), but they give no hint of such steps elsewhere in Tibet.

Second, because the recordings clearly show lateral heterogeneity within the crust, it is reasonable to expect there to be lateral heterogeneity in the crust–mantle transition. Because the nature of that transition affects the strength of wide-angle reflections, the absence of a signal at a distance of 250 km could be caused by variations in the structure near the Moho, which nevertheless lies at a relatively uniform depth.

The dependence of the strength of the reflection on the velocity gradient at the Moho is shown most clearly by synthetic seismograms (figure 4 of Hirn *et al.* 1984*c*) for a set of plausible transitions at the crust–mantle interface. For the profile south of the Indus–Tsangpo Suture, it was necessary to postulate a very thick transition zone (12 km) between the crust and mantle beneath this area. For an abrupt step in velocity at the same depth, centred at 76 km, the strongest wide-angle reflections would be recorded at distances less than 200 km. For a shallower Moho, these signals would be strong at yet shorter distances. Most, but not all, seismograms from the fan profiles were recorded at distances between 200 and 250 km, but they are corrected for distance and plotted (figure 5; figure 2 of Hirn *et al.* 1984*c*) so that reflections from the same depths are aligned. Hirn *et al.* (1984*b*) noted that such corrections are based on the assumption that the velocity structure of the crust is the same everywhere and that 'the largest uncertainty in the conversion of time into depth results from the lack of control on possible variations in the velocity contrast across the Moho along the section'. For me, this uncertainty, coupled with the likely possibilities that the velocity structure of the Moho beneath Tibet is variable and that the unusually thick transition south of the suture does not prevail throughout Tibet, casts doubts on the inference of 20 km steps in the Moho.

PHILOSOPHICAL TRANSACTIONS OF THE ROYAL SOCIETY A MATHEMATICAL, PHYSICAL & ENGINEERING SCIENCES

My comments here are not meant to be a criticism of the work done by Hirn *et al.* (1984*b*), of the experimental design, of the field investigation, or of their analysis. Nor do I assert that their inferences of steps in the Moho or of major thrust faults offsetting it are incorrect. Nevertheless, I think that their presentation of their data is inadequate to allow the reader to decide whether the inferred steps and steep dips of the Moho are required. Thus, I conclude that data from explosion seismology show a complex crustal structure, with dipping interfaces that could well be the manifestations of major thrust faults; but for the area north of the Indus–Tsangpo Suture Zone, I do not think that these results prove that the Moho lies at a depth less than about 65 km.

Surface-wave propagation across Tibet

Introduction. The velocities of seismic surface waves can provide important constraints on the seismic wave velocity structure of large areas (at least several hundred kilometres in dimension) such as Tibet, but for the non-seismologist there must seem to be numerous obstacles to appreciating these constraints. An intuitive understanding of the analysis and interpretation of surface waves is much more difficult to grasp than that of travel times of body waves. First, the waves are dispersed with longer periods being more sensitive to deeper structure and, in general, travelling faster than shorter periods. Second, the velocities can be described in two ways. Phase velocities describe the velocity of a wave train with a specific period. They are more difficult to measure but contain more information than group velocities, which describe the velocity of a packet of waves spanning a narrow range of periods. Third, there are two types of surface waves, Rayleigh and Love waves, both of which depend primarily on the shear-wave velocity in the Earth, but in different ways. Fourth, for a region the size of Tibet, where until recently all nearby permanent long-period seismographs have lain outside the plateau, isolating the portion of the path within Tibet has been a serious problem. Finally, even when reliable surface-wave velocities exist, the non-uniqueness of the constraints that they impose on the Earth structure is often obscured in the presentation of the results; all too often only one model that fits the data is shown, leaving the reader at a loss as to how to decide what other structures also are allowed by the data.

Most early studies of Tibet considered only group velocities of Rayleigh waves, and such studies, by themselves, did not place tight constraints on the crustal thickness or the shear-wave velocity in the upper mantle. This is illustrated clearly by two experiments: one inadvertent and the other specifically addressing Tibet.

In the 1950s, Maurice Ewing and Frank Press measured low Rayleigh-wave phase velocities for paths across the Basin and Range Province of the western United States, where a broad area of high elevation is associated with large negative Bouguer gravity anomalies that indicate an overall state of isostatic equilibrium. They concluded that the crust beneath the Basin and Range Province is thick and noted the following. 'The correlation of phase-velocity variations with crustal-thickness changes is justified, and permits specification of the mechanism of (isostatic) compensation as the regional Airy system' (Ewing & Press 1959). Whereas this conclusion is correct for most of the Earth, the Basin and Range Province looms as the Earth's most glaring example of where Airy's model of isostasy fails, for the crust is thinner, not thicker, than normal in that region. Recognizing both that none of the scientists who have studied surface-wave dispersion across Tibet have attained the stature of either Ewing or Press, and that until the 1980s surface-wave phase velocities for Tibet could not be measured as reliably as those for western United States in 1959, readers should be very cautious about believing many of the inferences drawn solely from early studies of surface-wave dispersion across Tibet.

In presenting surface-wave group velocities for Tibet, Bird (1976) and Chen (1979; Chen & Molnar 1981) compared them with calculations for different crustal thicknesses and for different shear-wave velocities in the uppermost mantle (Sn velocities). The measured dispersion curves could be matched satisfactorily by structures with crustal thicknesses between 55 and 85 km, for different, but reasonable, Sn velocities. Thus for group velocities to provide a tight constraint on the crustal thickness, not only must the dispersion curve be measured accurately, but also the Sn velocity should be obtained independently.

To some extent this non-uniqueness associated with group velocities is removed by accurate measurements of phase velocities at sufficiently long periods, but the study of phase velocities across Tibet required the development of techniques to circumvent the absence of long period seismographs on both sides of the plateau (Patton 1980*a*; Romanowicz 1982) or the (temporary) installation of long period seismographs within Tibet (Jobert *et al.* 1985). Although studies by Brandon & Romanowicz (1986), Jobert *et al.* (1985) and Romanowicz (1982) provide relatively tight constraints on the crustal and upper-mantle structure, these studies not only have considered relatively small portions of Tibet. Moreover, they demonstrate clear lateral heterogeneity in the structure. Consequently, I also review briefly the less-definitive work based on group velocities, which covers parts of Tibet not studied with phase velocities.

Group velocities. Among the many studies of surface-wave dispersion across Tibet, a relatively small area to be studied with surface waves, two approaches have been taken in gathering data.

Most studies used long paths for which the portion beneath Tibet itself was less than 70% of the overall path (Chun & Yoshii 1977; Feng 1982; Feng & Teng 1983; Gupta & Narain 1967; Patton 1980*b*; Pines *et al.* 1980; Tung & Teng 1974). The first such study (Gupta & Narain 1967) used paths for which Tibet constitutes only 10% of the path. Clearly, to isolate the part of the path appropriate for Tibet, it was necessary to know, or to assume, the dispersion appropriate for paths outside of Tibet. Some later studies used numerous multiple paths and solved simultaneously for dispersion curves in different areas (Chun & McEvilly 1986; Feng 1982; Feng & Teng 1983; Patton 1980*b*), but for most such studies, it is difficult to know both how well resolved the dispersion curves for Tibet are and, given the existence of lateral heterogeneity, what are the precise regions represented by those curves.

All of these studies show that surface waves are delayed significantly when paths cross the Tibetan Plateau, and all reported crustal thicknesses of about 70 km and low shear-wave velocities (4.4–4.5 km s^{-1} or less) for the mantle immediately below the Moho. Because these upper-mantle velocities are distinctly lower than those determined by using travel times of Sn (discussed below), these inferences of a thick crust must also be viewed with scepticism.

The other approach to determining dispersion curves for Tibet has been to consider, in so far as possible, paths confined to the plateau. Initially this approach was realized by the analysis of surface waves from earthquakes in or on the margins of the plateau recorded at stations close to the edge of the plateau (Bird 1976; Chen 1979; Chen & Molnar 1981). The principal disadvantage of this approach has been that there have been few earthquakes sufficiently large, without being too large, and in appropriate locations to define the entire dispersion curve for periods between 20 and 90 s. Chen relied primarily on Rayleigh-wave group velocities measured for two paths, one from northeast Tibet to New Delhi and the other from the Pamir across southern Tibet to Shillong (figure 4). Chen's data, coupled with Sn velocities determined independently (and discussed below), were sufficient to show that the average crustal thickness for Tibet is about 70($\pm$5–10) km.

Recently, Chun & McEvilly (1986) presented group velocities for both Rayleigh and Love waves crossing Tibet, determined by comparing measured values for paths with different fractions across Tibet and by extrapolating to paths purely across Tibet. Implicit in this exercise was the assumption that for each period and for each path, the velocity is the same throughout the area traversed by these paths outside of Tibet. They obtained very low group velocities in the period range from 25 to 45 s, and they inferred a zone of very low velocities within the crust. They also inferred a crustal thickness of 74 $\pm$ 10 km and an uppermost mantle shear velocity of 4.50–4.55 km s^{-1}, but they did not show whether their data also allow a thinner crust and a higher upper-mantle velocity.

Phase velocities. In my opinion, the most definitive studies of surface-wave dispersion across Tibet are those of Brandon & Romanowicz (1986), Jobert *et al.* (1985), Patton (1980*b*) and Romanowicz (1982), who determined phase velocities for surface waves across parts of Tibet. Except for relatively short periods, the first phase velocities measured for the Tibetan Plateau were determined by Patton (1980*b*), using earthquakes northwest of Tibet and recorded at stations in southeast Asia and the Philippines. Some arbitrariness was required both to assign boundaries to regions with different structures and then to decide how much of each path should be assigned to which province. Given the existence of lateral heterogeneity within Tibet and the likelihood that paths crossing the margins of Tibet will be refracted and will not follow great circles, I have greater doubts about dispersion curves determined by such regionalization than those determined by using strictly pure paths. Nevertheless, the measurements obtained later by Romanowicz (1982) lie within the uncertainties quoted by Patton (1980*b*) and clearly give credibility to his analysis.

Romanowicz (1982) used pairs of earthquakes that lie along great circles passing very close to stations in opposite directions from Tibet. She first measured dispersion curves for each earthquake at each station. Then for each station, in essence, she took the differences in propagation times for phases from the two earthquakes and obtained average phase velocities for the portion of the paths between the earthquakes and within Tibet. Thus although the structure between the earthquakes and for which the dispersion curve was obtained need not be laterally homogeneous, she could avoid the risky assumptions that are necessary in regionalizing paths that do not follow the same great circles.

Romanowicz (1982) determined phase velocities for both Rayleigh and Love waves, and thus obtained tighter constraints on the structures than had been possible. Her data could not be fitted with most previously published structures, but they corroborated the necessity of both a thick crust of about 65–70 km and a high Sn velocity of about 4.65–4.7 km s^{-1} (figure 6). The agreement between the structures inferred by Chen and by Romanowicz is, in fact, somewhat surprising because the paths that Chen studied were principally in the southern and western parts of the high plateau, but hers cross the northern and the eastern parts of Tibet (figure 4). The lower elevations of eastern Tibet are likely to be compensated by thinner crust than that beneath the high parts of the plateau, where Chen concentrated his study.

Jobert *et al.* (1985) installed a temporary array of four seismographs in southern Tibet, from

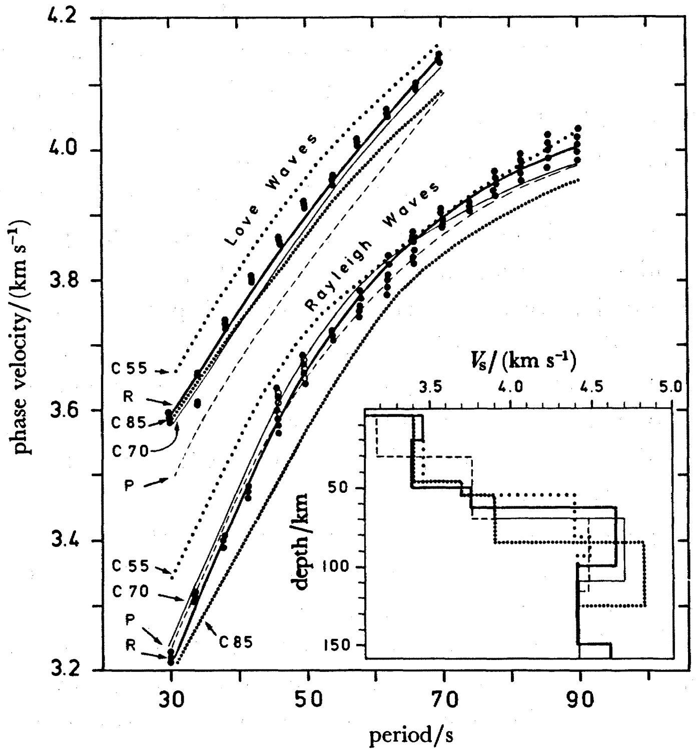

Figure 6. Comparisons of Romanowicz's (1982) observed and calculated Rayleigh- and Love-wave phase-velocity dispersion curves showing both poor and satisfactory agreement, and corresponding shear-wave velocity structures. Points show measurements, with the higher velocities defining the curve for Love waves and with the lower velocities for Rayleigh waves. The path used to measure the phase velocities crosses northern and eastern Tibet (figure 4). The dispersion curves calculated for Romanowicz's (1982) structure are labelled R. Note that Chen & Molnar (1981) could not rule out crustal thickness of 55 km (curve C55) or 85 km (curve C85) with group velocities alone, but phase velocities do not permit such average crustal thicknesses. Patton's (1980*b*) proposed structure, P, based solely on Rayleigh waves, can be rejected only because of a poor fit to Love waves. (Redrawn from Romanowicz 1982.)

300 to 580 km apart, surrounding Lhasa, and spanning the Indus–Tsangpo Suture Zone (figure 4). They measured phase velocities for four separate paths, and for two cases they reported measurements for the relatively long periods of 150 s. The velocities for periods less than 100 s require a thick crust, about 70 km but not as much as 80 km. On the basis of the dispersion of the longest periods, 100–150 s, they inferred a thin (30 km) high-velocity layer overlying a low-velocity zone in the mantle beneath their array. I suspect, however, that because their array would span only one wavelength at these long periods, uncertainties both in the phase velocities and in the assumption of lateral homogeneity do not permit the resolution of the shear velocity below a depth of about 100 km.

In an extension of Romanowicz's (1982) study but using more paths, Brandon & Romanowicz (1986) compared Rayleigh-wave phase velocities across north–central and northernmost Tibet. They corroborated Romanowicz's (1982) measurements for the western 70% of the path that she had studied across the northernmost part of Tibet. Despite a large scatter, measured phase velocities for shorter paths across north–central Tibet and for periods between 30 and 60 s (figure 7) are consistently larger than those for the paths across northernmost Tibet. These different phase velocities require a thinner crust for north–central Tibet (50–60 km) than for the rest of Tibet (65–70 km) but with a lower upper-mantle shear

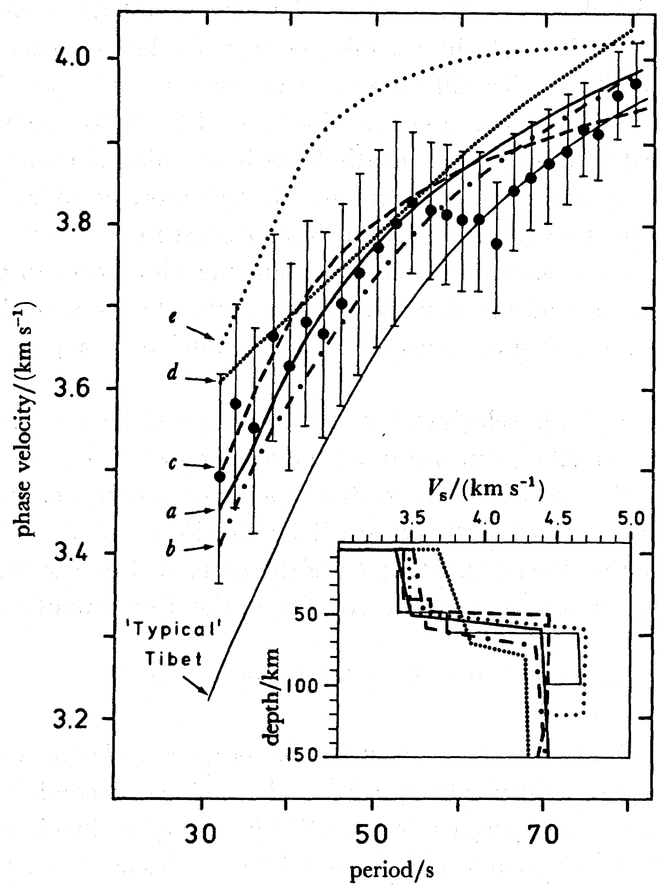

FIGURE 7. Comparisons of Brandon & Romanowicz's (1986) observed phase velocities for short paths across north–central Tibet (figure 4) and calculated curves for layered structures yielding both satisfactory and unsatisfactory fits. 'Typical Tibet' corresponds to curve R in figure 6. Note the good fits for structures *a*, *b*, and *c* with thinner crusts (50–60 km) than normal for Tibet and with lower-mantle S-wave velocities (4.5 km s^{-1} or less), but poor fits for structures with a crust thick as 65 km (*d* and 'Typical Tibet') or with uppermost-mantle velocities higher than 4.5 km s^{-1} ('Typical Tibet' and *e*). (Redrawn from Brandon & Romanowicz 1986.)

velocity (4.4 km s^{-1} or less) than elsewhere beneath Tibet (about 4.65 km s^{-1}). If the crust were nearly as thick as elsewhere (65 km), then the shear velocity in the uppermost mantle must be low (*ca.* 4.4 km s^{-1}) or the average shear-wave velocity in the crust must be distinctly higher than elsewhere in Tibet (figure 7). They stated that a high uppermost mantle shear velocity (4.6 km s^{-1} or more) can be ruled out. Thus the structure of north–central Tibet (or of Chang Thang) must be very different from that to the north and east, from that determined by Jobert *et al.* (1985) for southernmost Tibet, or from the average for southern and western Tibet, determined from group velocities and Sn travel times (Chen 1979; Chen & Molnar 1981).

In my opinion, the differences in the structures cannot be isolated and resolved well enough to prove both that the crust is much thinner (15 km) instead of only slightly thinner (5 km) than elsewhere in Tibet, and that the S-wave velocity in the mantle is much less (only 4.4 km s^{-1}) than that elsewhere (4.7 km s^{-1}), instead of only slightly less (4.55 km s^{-1}). Brandon & Romanowicz's (1986) results, however, do not seem to allow only slight differences in both crustal thickness and upper-mantle shear-wave velocity. As discussed below, my suspicion is that the crust is slightly thinner (by 5 km or at the most 10 km) than beneath most of the plateau, but the shear velocity is distinctly lower than elsewhere.

Summary. Both group and phase velocities of Rayleigh waves and Love waves are delayed along paths crossing Tibet. The low velocities require a crustal thickness in excess of 50 km, and for most regions in excess of 60 km. Crustal thicknesses in excess of 80 km can be ruled out for all paths studied, and for most of Tibet, a crustal thickness of 65–70 km seems required.

Clear evidence for lateral heterogeneity beneath Tibet is provided not only by body waves (discussed below) but also by surface waves (Brandon & Romanowicz 1986), which show an area of lower uppermost shear-wave velocity and thinner crust in north–central Tibet than elsewhere in the plateau. These variations might explain the differences in group velocities measured by different workers, and the different structures that they deduced, but if so, they also render the regionalization of surface-wave dispersion into arbitrary tectonic provinces risky.

Although Rayleigh-wave phase velocities can resolve large differences in upper-mantle velocities for regions the size of Tibet, constraints on these velocities are best derived from body waves. Thus, with the exceptions of Brandon & Romanowicz's (1986) detailed investigation of north–central Tibet, the study of southernmost Tibet by Jobert *et al.* (1985) and that of Romanowicz (1982) for the northeasternmost part of the plateau, I do not think that surface waves have placed an important bound on the velocity in the upper mantle beneath Tibet.

Upper-mantle structure of the Tibetan Plateau

Introduction

P-wave and S-wave velocities in the uppermost 200 km of the mantle are commonly used to distinguish regions with a particularly cold upper mantle, such as Precambrian shields, from regions with a particularly warm uppermost mantle. Shields are typically characterized by Pn and Sn velocities of 8.1 km s^{-1} or greater and about 4.7 km s^{-1}, respectively. Pn velocities less than 8.0 km s^{-1} are typical of regions with high heat flow such as the Basin and Range Province of the western United States (see, for example, Black & Braile 1982) and shear-wave velocities of 4.5 km s^{-1} and lower are typical of the low-velocity zone in the upper mantle, where partial melting is likely.

The Indian Shield is underlain by a thick high-velocity zone. Pn and Sn phases propagate with velocities of 8.4 and 4.7 km s^{-1}, respectively (Huestis *et al.* 1973; Ni & Barazangi 1983), and waveforms of SH phases show that the high-velocity layer is thick (*ca.* 200 km) (Lyon-Caen 1986). Thus, if Argand's (1924) hypothesis that India underthrusted the whole of Tibet were correct, then one might expect to find Tibet underlain by a structure similar to that beneath India.

Showing the presence or absence of shield structure beneath Tibet has been difficult, because although the Pn and Sn velocities are high, it has been difficult to measure the thickness of the region characterized by such velocities. For regions the size of entire continents, surface-wave phase velocities at long periods (100 s or more) can resolve thick high-velocity lids on minor low-velocity zones or pronounced low-velocity zones without lids, but, with the possible exception of the study of Jobert *et al.* (1985), phase velocities, and especially group velocities, of surface waves across Tibet have not been measured at sufficiently long periods to resolve such deep structure.

In this section, I review three types of studies using body waves to constrain the upper-mantle structure of Tibet: (1) measurements of Pn and Sn arrival times for earthquakes in different parts of Tibet, which yield estimated P-wave and S-wave velocities in the uppermost mantle; (2) differences in S-wave and P-wave travel times from earthquakes in Tibet and the Himalaya recorded at teleseismic distances, which yield constraints on the average shear wave velocity in the upper several hundred kilometres of the mantle beneath Tibet; and (3) travel times and waveforms of SH phases for paths beneath Tibet and recorded at regional distances, which place constraints on the depth distribution of material with different velocities.

Propagation of Pn and Sn across the Tibetan Plateau

Three studies have reported Pn velocities for Tibet, and two of them Sn velocities. For each, the arrival times of these phases from earthquakes in different parts of Tibet and recorded at different distances from recording stations within or near Tibet were used to construct travel time curves (figure 8). Chen & Molnar (1981) used reported arrivals at the station in Lhasa;

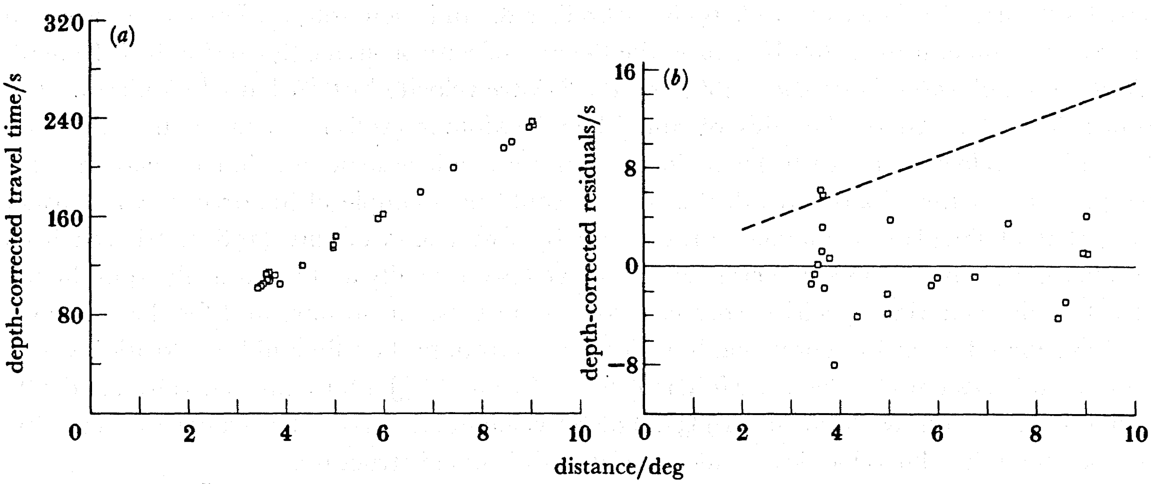

FIGURE 8. Plots of Sn (3–10°) travel times (*a*) and residuals (*b*) about the best fitting linear travel-time curve against distance from earthquakes within the Tibetan Plateau to the station at Lhasa (figure 4). Velocity = 4.77 ± 0.8 km s^{-1}. The broken line in (*b*) shows slope of travel-time curve if the velocity were 4.5 km s^{-1}. *N* is the number of arrival times used; in (*b*) = 23. All origin times were normalized to a common focal depth of 33 km, reducing travel-time differences (scatter) arising from erroneous focal depths and correspondingly erroneous origin times. (From Chen & Molnar 1981.)

Jia Su-juan *et al.* (1981) measured arrival times of Pn at Lhasa and at stations east of the plateau in China; and Ni & Barazangi (1983) measured arrival times at stations of the World-Wide Standardized Seismograph Network (WWSSN) in India and Pakistan. Arrival times measured by Jia Su-juan *et al.* (1981) and by Ni & Barazangi (1983) are probably more reliable than those taken by Chen & Molnar (1981) from bulletins, but there is overall agreement in Pn and Sn velocities: 8.12 ± 0.06 km s^{-1} and 4.77 ± 0.08 km s^{-1} (Chen & Molnar 1981); 8.11 ± 0.04 km s^{-1} for Pn (Jia Su-juan *et al.* 1981); and 8.42 ± 0.10 km s^{-1} and 4.73 ± 0.06 km s^{-1} (Ni & Barazangi 1983). Paths confined to Tibet may yield less scatter than those for which different path lengths lie outside of Tibet, and the relatively high Pn velocity of Ni & Barazangi (1983) might be a consequence of the smaller fractions of their paths beneath Tibet. The agreement of the measured Sn velocities, however, does not support this inference. Finally, Chen & Molnar (1981), but not Ni & Barazangi (1983), found that adjustments to origin times for different reported focal depths reduced the scatter in travel-time curves.

PHILOSOPHICAL TRANSACTIONS OF THE ROYAL SOCIETY A MATHEMATICAL, PHYSICAL & ENGINEERING SCIENCES

The apparent velocities of both Pn and Sn are similar to those of shields and markedly different from areas characterized by high heat flow. Barazangi & Ni (1982; Ni & Barazangi 1983) made the step of concluding that Tibet is underlain by a shield structure, but caution should be exercised before accepting this inference.

First, because of curvature of the Earth, waves refracted at deep levels will yield higher apparent velocities than those refracted at shallower depths in material of the same velocity. For a Moho 35 km deeper than normal the apparent velocities should be 0.55% higher than normal (Chen & Molnar 1981).

Second, an increase in pressure increases the material velocity. A difference in crustal thickness of 35 km corresponds to a higher pressure of about 1 GPa at the same distance below the Moho. For Olivine (forsterite) this would cause an increase in the P-wave velocity of 0.1 km s^{-1} (Anderson *et al.* 1968; Schreiber & Anderson 1967*a*) but in the S-wave velocity of only 0.025 km s^{-1} (Anderson *et al.* 1968; Schreiber & Anderson 1967*b*). For comparison, an increase in temperature of 250 K reduces the P-wave velocity of olivine (forsterite) by 0.1 km s^{-1} (Anderson *et al.* 1968; Soga *et al.* 1966) and the S-wave velocity by 0.07 km s^{-1} (Anderson *et al.* 1968; Soga *et al.* 1966). For this reason, Chen & Molnar (1981) concluded that the high Pn and Sn velocities beneath Tibet do not require a shield structure, but instead that the temperature at the Moho beneath the plateau could be a couple of hundred kelvin warmer than that of shields, an inference drawn also by Chun & McEvilly (1986). Viewed from another perspective, if 35 km of crust were removed isothermally and isostatically from the top of Tibet, the material velocities, corrected for the decrease in pressure and for the shallower depth of the refractor but corresponding to the various published Pn and Sn velocities, would be 7.98 and 4.72 km s^{-1} (Chen & Molnar 1981), 7.97 km s^{-1} (Jia Su-juan *et al.* 1981), and 8.27 and 4.68 km s^{-1} (Ni & Barazangi 1983). The Sn velocities and Ni & Barazangi's Pn velocity, but not the other Pn velocities, would accord with a shield structure.

The greatest risk in using the Pn and Sn velocities to infer that Tibet is underlain by a shield-like upper mantle arises from the lack of constraints that measurements of Pn and Sn phases place on the thickness of the layer with such a velocity. The existence of relatively high Pn and Sn velocities does not rule out the possibility that the mean velocities in the upper 300 km of the mantle are low and that a thick, pronounced low-velocity zone exists.

Thus, measurements of Pn and Sn velocities beneath Tibet are relatively high; some of them are consistent with a shield-like structure beneath Tibet, but they do not require such a structure.

S–P travel-time differences

To constrain the average shear-wave velocity structure in the upper mantle beneath Tibet, Chen & Molnar (1981; Molnar & Chen 1984) measured S-wave and P-wave arrival times to distant stations (30° or less) from earthquakes in Tibet and the Himalaya (see also Pettersen & Doornbos 1987). With accurate focal depths, determined from the synthesis of P phases (Baranowski *et al.* 1984; Molnar & Chen 1983), corrections for erroneous origin times associated with erroneous focal depths given by the International Seismological Center, allowed the determination of travel times of P and S phases. To reduce the scatter in S-wave travel times, differences in S-wave and P-wave travel times were considered, because at stations where one phase is delayed or advanced, usually the other is as well. Finally, Chen & Molnar considered earthquakes in both Tibet and the Himalaya so that a comparison between the structures beneath the two areas could be made, and so that delays or advances introduced by the different structures near the receivers could be further minimized.

Travel-time differences between S-waves and P-waves from earthquakes in the Himalaya deviated by -1.95 s to $+0.65$ s from Jeffreys & Bullen's (1940) travel times, after correcting for the crust being somewhat thicker than normal beneath the Himalayan earthquakes (figure 9). If Herrin's (1968) more recent P-wave travel times were used, then S–P travel-time differences would be 2–4 s smaller than normal, which concurs with the Himalaya being underlain by a shield-like structure (see discussion of the Himalaya, below).

S–P travel-time differences from Tibetan earthquakes are typically 2–5 s larger than those for the Himalaya, again after correcting for the thick crust of Tibet (figure 9). The largest

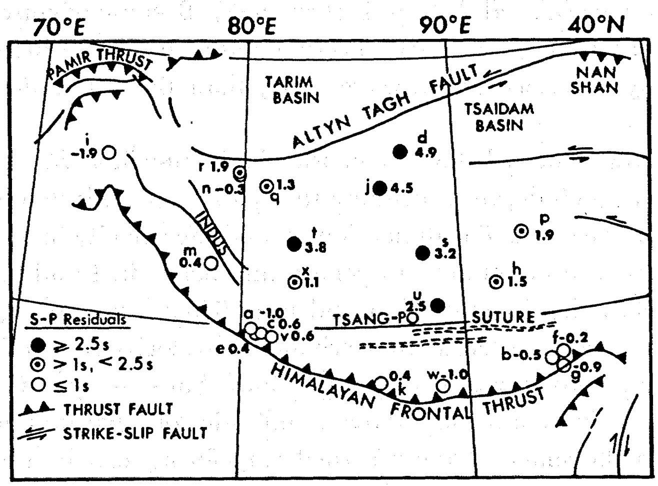

FIGURE 9. Map of earthquakes and mean S–P travel-time residuals to stations 30–80° from them. Times are in seconds and include corrections for excess crustal thickness beneath the Himalaya and beneath Tibet. Residuals were obtained from Jeffreys & Bullen's (1940) P-wave and S-wave travel times. If Herrin's (1968) P-wave travel times were used, the values would all be about 2 s less. Note the large residuals, corresponding to late S-waves, from earthquakes in northern and central Tibet. (From Molnar & Chen 1984.)

differences are from earthquakes in north–central Tibet, a result corroborated by Petterson & Doornbos (1987) for more recent earthquakes. S–P intervals from three events in central Tibet are 2.5–4.5 s greater than those predicted by Jeffreys & Bullen's (1940) tables, or 0.5–2.5 s greater than those calculated from Herrin's (1968) P-wave times, also corroborated by Pettersen & Doornbos (1987). If such differences were caused by differences in shear velocities in the upper 250 km of the mantle beneath Tibet and the Himalaya, then the mean shear-wave velocity beneath central Tibet would be 4–8 % lower than that of the Himalaya. Smaller differences in S–P intervals from earthquakes in western, southern, and eastern Tibet than from Himalayan earthquakes imply average velocities 2–3 % less than those of the Himalaya (Molnar & Chen 1984). A 2 % difference would be only 0.1 km s^{-1} which is not very significant, but 4 % and 8 % differences correspond to 0.2 and 0.4 km s^{-1}, which would require a thin high-velocity lid over a thick low-velocity zone beneath Tibet. Thus, in so far as these results apply to the uppermost mantle, they imply that a shield-like structure could underlie only the margins of Tibet.

The weakness of S–P travel-time intervals as a constraint on the upper-mantle velocity beneath Tibet lies in the assumption that the S-waves from earthquakes in Tibet are delayed in the uppermost mantle and not at greater depth beneath Tibet.

Travel times and waveforms of SH phases

To investigate variations in seismic-wave velocities with depth in the upper several hundred kilometres of the mantle requires an analysis of phases that penetrate to varying depths in this range. Because of the low-velocity zone and because of rapid increases in velocity near depths of 400 and 650 km, travel times for rays that bottom at 100, 400 and 700 km are comparable to one another. Thus phases travelling along these different paths combine to make relatively complicated signals at distances of 15–25° from the sources, and, in general, the different arrivals can be distinguished and identified only by synthesizing seismograms and comparing them with observed signals (Grand & Helmberger 1984). Because of conversions of vertically polarized S-waves to and from P-waves at reflecting and transmitting interfaces, it is easier to work with horizontally polarized shear waves, SH, than the yet more complex vertically polarized SV.

Clearly a high or a low velocity below the depth of 400 km will advance or delay only those signals that penetrate to such depths, but those that pass above this depth will be unaffected by the velocity structure below it. The dimensions of and the velocity in a shallow low-velocity zone will affect the arrival times of all rays penetrating below it. In addition, because waves refracted both just below depths of 400 km and near 650 km are strongly focused at some distances, the velocity of the material in an overlying low-velocity zone affects the distances at which these signals are recorded with strong amplitudes. Thus, as Lyon-Caen (1986) showed, both the relative arrival times and the relative amplitudes of separate phases, both of which manifest themselves in the shape of the recorded waveforms, can be used to constrain the upper-mantle velocity structure of an area the size of Tibet.

Lyon-Caen's (1986) procedure was first to examine paths across India, to establish that it is underlain by a shield structure, and then to consider Tibet. For epicentral distances of 10–20°, the first signals to arrive pass through the uppermost mantle, above the low-velocity zone. Their arrival times corroborate the existence of high-velocity layers beneath both India and Tibet. A plot of travel times for paths crossing Tibet, however, reveals delays of 5–12 s for rays reflected at the velocity increase at a depth of about 400 km, of which only 4 s can be attributed to the thicker crust of Tibet than India (figure 10). The greater delays imply the existence of lower velocities in the mantle beneath Tibet at depths shallower than 400 km.

Such delays are perhaps best illustrated by a comparison of SS phases that are reflected beneath Tibet and beneath India recorded at epicentral distances of 35–45° (figure 11). At these distances, the direct S-wave penetrates the lower mantle, but the first large signal comprising SS is reflected at 400 km depth. A comparison of the differences in arrival times of SS and S thus provides a strong constraint on the average velocity above 400 km. The SS phase bouncing off the Earth's surface beneath Tibet is delayed 25 s from that bouncing beneath India, an extremely large delay. Roughly half of this delay can be attributed to Tibet's thick crust, but at least 12 s of it in the mantle implies that the average S-wave velocity shallower than 400 km is at least 3% less than that beneath India.

SH phases from earthquakes in the Tien Shan and passing beneath Tibet to stations in India are not delayed (squares in figure 10). These rays do not sample the upper 250 km of Tibet, but they do pass through the mantle at depths between 250 and 660 km beneath Tibet. In

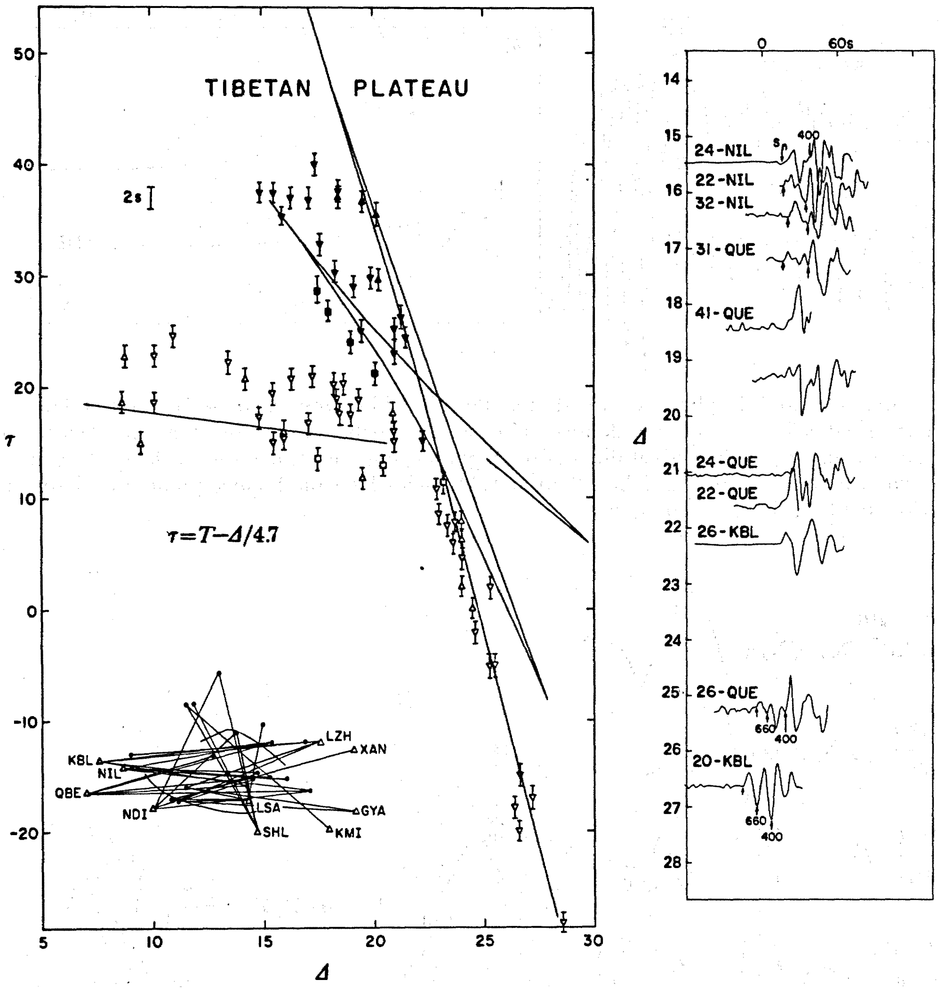

FIGURE 10. Travel times of SH phases against distance for paths across the Tibetan Plateau (left) and examples of seismograms recorded at various distances (right). Different symbols illustrate different paths: upright triangles for recordings at LZH, XAN and LSA, inverted triangles for recordings at KBL, QUE, NDI, KMI, and GYA for roughly east–west paths, and squares for north–south paths (see map in lower left). Open symbols show first arrivals, and closed symbols show later arrivals. Lines show the travel time curves derived by Lyon-Caen (1986) for the Indian Shield but delayed 8 s for the Sn branch and 4 s for other branches to account for the thick crust of Tibet. Note that most arrivals reflected from or refracted just below the 400 km discontinuity (recorded at distances between 15 and 20°) are late, but those from earthquakes in the Tien Shan to stations in India (dark squares) are early; these latter paths pass below the plateau at depths of 250 km or more. (From Lyon-Caen 1986.)

particular, signals reflected at 400 km beneath Tibet arrive at the same time as similar phases travelling only beneath the Indian Shield (figure 12). Thus they too imply that the mantle deeper than about 250 km beneath Tibet is not unusual.

Most of the seismograms shown in figures 10, 11 and 12 sampled the northern part of Tibet, and one might suspect that Lyon-Caen (1986) has shown that a shield structure is absent only from the northern part of Tibet. Notice, however, that the SH phase from an earthquake in central Tibet travelling south to HYB (15-HYB in figure 12) through the uppermost mantle of southern Tibet and bottoming at 400 km is markedly delayed, by almost as much as the signal from an event in northern Tibet to QUE (28-QUE in figure 12). Moreover, notice that the waveform at KOD from this event in central Tibet, which consists of phases refracted

PHILOSOPHICAL TRANSACTIONS OF THE ROYAL SOCIETY A MATHEMATICAL, PHYSICAL & ENGINEERING SCIENCES

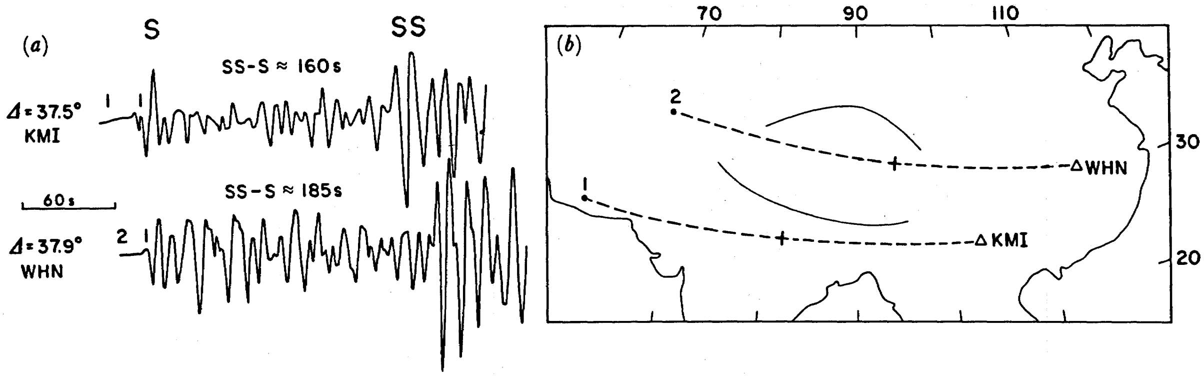

FIGURE 11. Examples of S and SS phases recorded at stations in China from earthquakes west of Tibet (*a*), (top) and (*b*) map of paths for these phases. Bounce points at the Earth's surface for SS are marked by plus signs. Seismograms are aligned at the arrival times of the S phases; note the much greater delay of SS at WHN, for which the bounce point is beneath Tibet, than at KMI, for which the bounce point is beneath the Indian Shield. (Modified from Lyon-Caen 1986.)

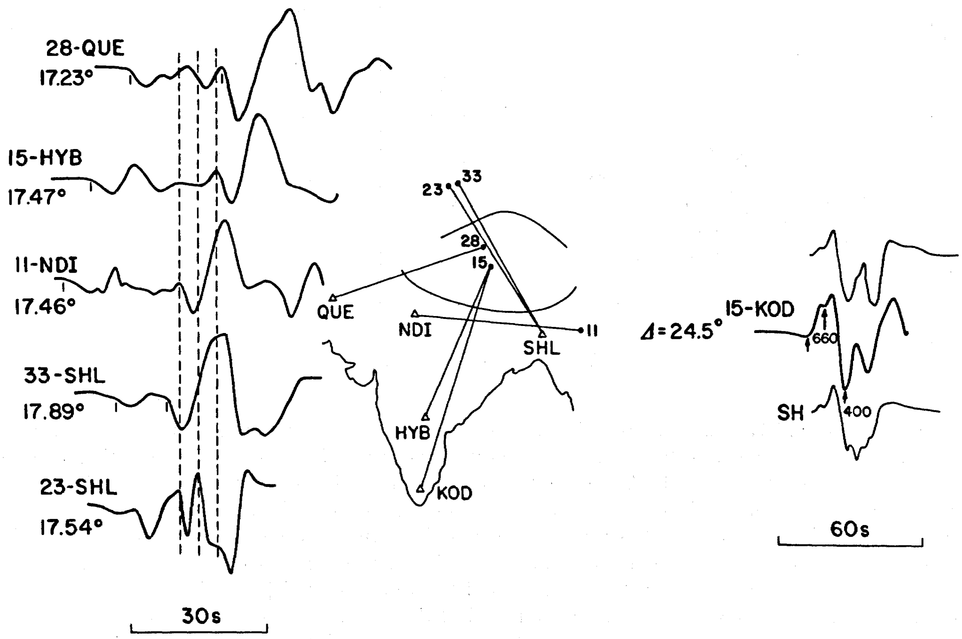

FIGURE 12. Comparison of SH phases recorded at a narrow range of distances for different paths shown on the map. On the left, seismograms are aligned by their reduced times: the measured time minus both the origin time of the earthquake and the epicentral distance divided by 4.7 km s^{-1}. The broken vertical lines are 4 s apart. The first tick marks the Sn phase, and the second tick marks the arrival from the 400 km discontinuity. The first broken line is aligned at the time of this latter arrival at NDI for the path (11-NDI) entirely across the Indian subcontinent. Note the prominent delays at QUE and HYB from earthquakes within Tibet, but the absence of delays at SHL for paths from earthquakes in the Tien Shan and for which rays pass deeper than 250 km beneath Tibet. This implies that the low-velocity material beneath Tibet is shallower than 250 km. On the right, the recorded SH phase from an earthquake within Tibet to KOD is compared with calculated seismograms for a shield structure (SH) and for one with a low-velocity zone shallower than 250 km (top). Seismograms are aligned at the times of refracted phases penetrating below a depth of 660 km and reflected phases from that depth. For a shield structure, the reflection from 400 km is calculated to arrive too early to be distinguished. With a low-velocity zone in the upper mantle, with the velocity equal to the mean of those deduced for Tibet and for a shield, this phase is clearly separate in the synthetic seismogram, and its arrival time correlates with a pulse on the observed seismogram. This suggests that at least part of southern Tibet is underlain by a well-developed low-velocity zone, and not by a shield structure. (From Lyon-Caen 1986.)

below 660 km, reflected at 660 km, and reflected at 400 km, cannot be matched with a shield structure (figure 12). A low-velocity zone in the upper mantle near the source is necessary to refract these rays differently and to cause a separation in the arrival times.

Thus despite the existence of a relatively high shear velocity in the uppermost mantle ($4.7\ \mathrm{km\ s^{-1}}$), at least the northern half, and possibly all, of the Tibetan Plateau is not underlain by a shield structure. Instead, the structure of the uppermost mantle beneath much of Tibet is more nearly that of the Basin and Range Province of the western United States than that of a stable continental region. A major uncertainty is the location of the transition from the thick low-velocity zone in north–central Tibet to the thick high-velocity zone that underlies the Indian Shield.

Lateral heterogeneity beneath the Tibetan Plateau

Seismic-wave velocities and attenuation

With increasing data of all kinds, the existence of lateral heterogeneity in the crust and upper mantle beneath Tibet has become increasingly clear. Seismic evidence can be interpreted as evidence for a zone of low velocity, and hence of high temperature, in the uppermost mantle beneath north–central Tibet. Less convincing evidence suggests that the coldest temperatures are beneath southern Tibet, excluding the Karakoram discussed below. Rayleigh phase velocities indicate both a thinner crust and a lower upper-mantle shear-wave velocity beneath north–central Tibet (Brandon & Romanowicz 1986) than beneath other parts of Tibet. The largest delays in S-waves, as reflected in S–P residuals (figure 9), are from earthquakes in north–central Tibet (Molnar & Chen 1984; Pettersen & Doornbos 1987), and Lyon-Caen's (1986) largest S-wave delays are also for paths across this part of Tibet. Finally, whereas Ni & Barazangi (1983) found high velocities of Pn and Sn for most of Tibet, Sn was not observed for paths crossing much of north–central Tibet (figure 13). Crudely, efficient and inefficient propagation are correlated with relatively cold and relatively hot uppermost mantle, respectively (see, for example, Molnar & Oliver 1969). Although the precise areas studied with these different techniques are not the same, and the areas of inferred low velocities and high attenuation also are not precisely the same, the overall coherency of the results is clear.

The existence of low velocities in the upper mantle beneath north–central Tibet is important because in this part of Tibet there is abundant evidence for late-Cainozoic volcanism (Burke *et al.* 1974; Deng 1978; Kidd 1975; Molnar *et al.* 1987*a*; Sengör & Kidd 1979). This volcanism includes both basaltic (Deng 1978) and very acidic material (Molnar *et al.* 1987*a*). The basaltic component suggests that an important mantle component is involved. The distribution of young volcanism is not yet well mapped, but the young cones visible on the *Landsat* imagery are confined to north–central Tibet.

There is a suggestion, from S-wave travel times (figure 9), that the average upper-mantle shear-wave velocities increase toward southern, western and eastern Tibet. Although there are too few earthquakes to allow one to contour mean S–P residuals from earthquakes in Tibet, the measured values increase smoothly away from north–central Tibet, where the events with the largest residuals occurred.

Lateral variation in temperature in the upper mantle

Two well-located earthquakes have occurred at depths of about 90 km beneath southern Tibet (Chen *et al.* 1981; Molnar & Chen 1983). Intermediate-depth earthquakes are very rare

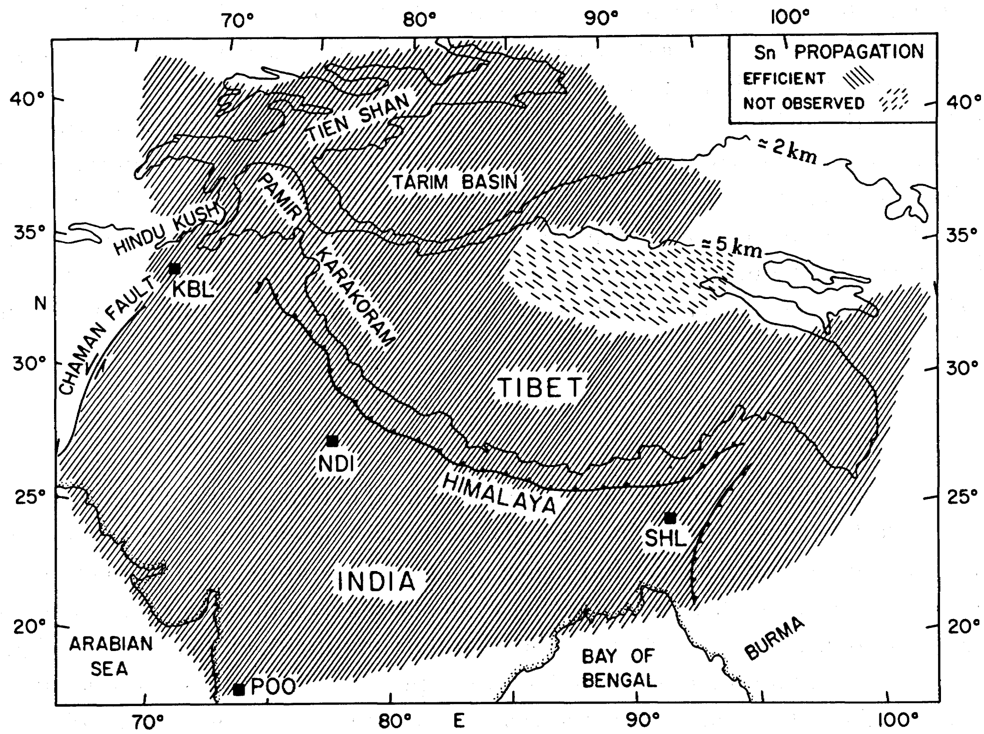

FIGURE 13. Map of the region in which the phase Sn propagates efficiently and inefficiently. Inefficient propagation implies the existence of a zone of low Q, or high attenuation. The boundary between areas of high and low Q is not sharply defined. Blank areas indicate areas with few or no observations. (From Ni & Barazangi 1983.)

except at active subduction zones, and Chen & Molnar (1983) infer that their existence implies temperatures of no more than 600–800 °C in the mantle, in this case at a depth of 90 km beneath Tibet. To my knowledge, except for the Karakoram, these are the only reliably located earthquakes at such depths beneath Tibet.

Clearly this evidence is insufficient to prove the existence of a smooth change in upper-mantle structure (and hence in temperature) from low velocities (and high temperatures) in north–central Tibet to higher velocities (and lower temperatures) in southern Tibet, but it seems likely that variations in velocity in the mantle would be smooth instead of abrupt, especially if they were caused by variations in temperature.

The lateral variations in upper-mantle shear velocity coupled with the remarkably uniform elevation of the plateau suggests that if isostatic equilibrium prevails, there must also be variations in crustal thickness. Therefore, in retrospect, the existence of relatively thin crust in north–central Tibet deduced by Brandon & Romanowicz (1986) ought not to be a surprise. It seems to me, however, that the differences in crustal thickness between north–central and southern Tibet cannot be more than 10 km. If the Moho in north–central Tibet were 500 K warmer than elsewhere beneath Tibet, and if lateral variations in the upper mantle were confined to the uppermost 200 km of the mantle, then the mean temperature difference would be 250 K. For a coefficient of thermal expansion of $3 \times 10^{-5}\ \mathrm{K^{-1}}$, the mean density in the uppermost mantle of north–central Tibet would be 25 kg m^{-3} less dense than that in southern Tibet, and a deficit of 5×10^{6} kg m^{-2} would exist in a column of mass in the mantle 200 km thick. For a density contrast of 500 kg m^{-3} at the Moho, this deficit could be compensated if the crust were 10 km thinner.

Note that although a temperature 500 K higher than that beneath southern Tibet is a large difference, it would correspond to a temperature of at least 1000 °C at the Moho beneath north–central Tibet, which is consistent with the partial melting of the mantle to form the basalt erupted at the surface.

Summary

The seismic data are broadly consistent with partial melting of the uppermost mantle of north–central Tibet, where recent volcanism has been observed. Correspondingly, there is no suggestion of such low velocities, and such high temperatures, in the mantle elsewhere beneath Tibet, for which late-Cainozoic volcanism has not been reported. The results are also consistent with a slightly thinner crust in north–central Tibet than farther south, suggesting that both Airy and Pratt isostasy share compensation for north–central Tibet's great height. Finally, the average shear-wave velocity in the upper mantle of southern Tibet seems to be higher than that in northern Tibet, but neither is the degree of difference well determined, nor is the location of the transition from one to the other well mapped.

Deep structure of the Himalaya

Introduction

When viewed on the scale of continent-sized objects, the Himalaya can appear as little more than the edge of the Tibetan Plateau. Despite the comparatively narrow width of the range, however, both the geologic history and the nature of the transition from the Precambrian shield of India to the very different structure of the plateau require that the Himalaya be treated separately from Tibet. The rocks comprising Tibet north of the Indus–Tsangpo Suture were already part of Asia before the collision with India, and those that form the Himalaya had been part of the separate continent of India. Thus unlike the other margins of Tibet where truly intracontinental deformation has occurred, the Himalaya lie as close, both in proximity and in meaning, to what might be called a plate boundary within a continent as can be found in Asia. In some oversimplified views, the Himalaya and Tibet might be said to lie on different plates. In any case, the imbrication of slices of India's ancient northern margin, as the leading edge of India was subducted beneath the southern margin of Asia, constitute a very different style and history of deformation from what has been found in Tibet. Thus, although the 40–50 Ma of intense tectonic activity have greatly altered the structure of both areas and the boundary between them, it is perhaps wise to begin by assuming their deep structures to be different.

The many tens to perhaps many hundreds of kilometres of underthrusting of India, first beneath southern Tibet and subsequently beneath slivers of India's own ancient northern margin, lead to the logical expectation that the crust thickens smoothly northward. Hirn *et al.* (1984*a*; Hirn & Sapin 1984), however, contend that the Moho may not be a smooth surface and suggest that it has been sliced by southward dipping thrust faults. In this context, the precise nature of the transition from a Moho at a normal depth beneath India to that at 70–75 km beneath southern Tibet is crucial for understanding how the range is supported. Let us first consider various studies of seismic waves from earthquakes, which are consistent with a smooth transition but do not prove it, then continue with the discussion of results from explosion seismology, which led Hirn, Lépine, Sapin and their colleagues to conclude that the

PHILOSOPHICAL TRANSACTIONS OF THE ROYAL SOCIETY A MATHEMATICAL, PHYSICAL & ENGINEERING SCIENCES

transition is not smooth, and finally turn to gravity anomalies, which may place constraints on the forces supporting the range, if the Moho is, in fact, a smooth surface.

Constraints from earthquake seismology on the deep structure of the Himalaya

The structure of Himalaya has not been studied in detail by using seismic waves from earthquakes, but what has been done is consistent with the structure of the Indian Shield extending beneath the Himalaya.

Fault-plane solutions and focal depths of earthquakes

The evidence most suggestive of this is provided by studies of moderate sized ($5.5 \leqslant$ magnitude $\leqslant 6.5$) earthquakes in the Himalaya (Baranowski *et al.* 1984; Ni & Barazangi 1984). Fault-plane solutions indicate thrust faulting with one nodal plane dipping gently north or northeast beneath the Himalaya and with the other nodal plane dipping steeply south or southwest away from the range. Clearly it is more sensible to assume that the gently dipping planes are the fault planes. For about half of the earthquakes studied, the plunge of the slip vector is less than 15°, suggesting underthrusting on very gently dipping planes. For the other half, it is between 20 and 35°, implying steeper dips of the thrust faults.

Focal depths for most of these earthquakes, below the Earth's surface, are about 15 ± 3 km (Baranowski *et al.* 1984; Ni & Barazangi 1984). Thus these earthquakes occur about 13 km below sea level or about 8 ± 3 km deeper than the depth of the basement of the Indian plate at the foot of the range, where about 5 km of late-Cainozoic sediment have been deposited. The dip of the basement of the Ganga Basin, at the front of the Himalaya is about 2–4°. If these earthquakes, which occur about 80–100 km north of the front of the range, occurred on the top surface of the Indian plate, the average dip of that surface beneath the Lesser Himalaya would be

$$\delta = \arctan\,(8 \pm 3\ \text{km}/90 \pm 10\ \text{km}) = 5 \pm 2°.$$

Thus both the focal depths and the fault-plane solutions of roughly half the major earthquakes are consistent with those earthquakes occurring on the top surface of the intact Indian Shield as it plunges beneath the Himalaya (Baranowski *et al.* 1984; Molnar & Chen 1982; Ni & Barazangi 1984).

Body-wave propagation beneath the Himalaya

Menke (1977) showed that the northward dip of the plate beneath the Himalaya is corroborated by increasingly delayed P-wave arrival times recorded at more northeasterly stations of the Tarbela array in Pakistan. Part of the delay is caused by higher elevations of the more northeasterly stations, but the remaining gradient in residuals is most simply explained by northeastward dip of the Moho of 4°. This direction is perpendicular to the trend of the range, and the amount is slightly larger than the dip of the basement beneath the neighbouring basin. Moreover, an inversion of relative arrival times across the Tarbela array for lateral heterogeneity in the crust and upper mantle reveals no evidence of other systematic variations in velocity in the mantle (Menke 1977).

Pn and Sn arrival times from earthquakes in the Himalaya and paths along the Himalaya yield high apparent velocities. For paths along the range to the Tarbela network in Pakistan, Menke & Jacob (1976) obtained Pn and Sn velocities of $8.50 \pm 0.35\ \text{km s}^{-1}$ and $5.00 \pm 0.19\ \text{km s}^{-1}$ respectively, but with a large scatter of more than 10 s in travel times. With more data and better located events, Ni & Barazangi (1983) obtained $8.48 \pm 0.05\ \text{km s}^{-1}$ and $4.75 \pm 0.05\ \text{km s}^{-1}$, which are not significantly different from corresponding velocities for the Indian Shield (or Tibet).

As discussed above, S-wave travel times from earthquakes in the Himalaya do not show significant delays (Chen & Molnar 1981; Molnar & Chen 1984). Depending upon whether one uses the P-wave travel times of Jeffreys & Bullen (1940) or Herrin (1968) to determine origin times of earthquakes and P-wave residuals, S-waves from Himalayan earthquakes arrive between 1 s late and 2 s early (figure 9), or between 1 s and 4 s early, relative to Jeffreys & Bullen's (1940) S-wave tables (Molnar & Chen 1984). These residuals are comparable with those at stations on some shields (Doyle & Hales 1967; Sipkin & Jordan 1975, 1980), and thus they are consistent with such a structure beneath the Himalaya. Similarly, Lyon-Caen (1986) found that both arrival times and waveforms of S-waves recorded in India from earthquakes in the Himalaya are consistent with a shield-like structure.

Among the results described in this section, none has the resolution to prove either that the entire Himalaya is underlain by a shield structure or that upper-mantle structure beneath the Himalaya is significantly different from that of India, but none give a hint of an important difference.

Constraints from explosion seismology on the deep structure of the Himalaya

Although numerous long seismic refraction profiles have been made in different parts of India (see, for example, Kaila 1982), no seismic refraction profile has been shot along the Himalayan chain. What information does exist on the velocity structure of the Himalaya is derived from one long unreversed profile that obliquely crosses the Himalaya (Beloussov *et al.* 1980; Kaila *et al.* 1978), from recordings of quarry blasts in the Kathmandu area (Pandey 1981), and from wide-angle reflections generated either by explosions in southern Tibet and recorded in Nepal (Hirn & Sapin 1984; Hirn *et al.* 1984*a*) or by local earthquakes recorded in Nepal (Pandey 1986). As I discuss below, some of these results have been interpreted as evidence that the Indian Shield does not extend far beneath the Himalaya, and these data deserve particular scrutiny.

The profile of Kaila et al. (1978) *across the Kashmir Himalaya*

Apparently, this profile, one of a series of profiles from the Tien Shan in the U.S.S.R. to Kashmir (Beloussov *et al.* 1980), was the first to use explosive sources and sufficient distances to record clear reflections from the Moho. The explosion used by Kaila *et al.* (1978) was detonated near Nanga Parbat at the western syntaxis of the Himalaya, and the unreversed profile crossed the Himalaya obliquely.

Kaila *et al.* (1978) inferred a steep, 15–20°, component of the dip of the Moho in the north–northwest direction of the profile, with the Moho reaching a depth of 70 km beneath the Greater Himalaya. They inferred an abrupt step of 5 km in the depth of the Moho just to the north of this locality, so that a maximum depth of 75 km was reached. They recorded no clear signals refracted by the underlying mantle. Because the profile is not reversed, the velocity structure of the crust cannot be constrained well, and the inferred depths of the Moho must surely be uncertain by at least several kilometres. Similarly the inferred dip of the Moho could be less if the velocity in the lower crust were greater than Kaila *et al.* (1978) assumed. Thus although a component of northward dip is probably inescapable, its value probably is not well constrained.

Wide-angle reflections beneath the Himalaya in Nepal

As discussed briefly above, Hirn and his colleagues carried out an extensive study of the structure of the area between the Indus–Tsangpo Suture Zone and the Greater Himalaya. I discussed these results above because an appreciation of their principal features was necessary for interpreting the seismograms that they obtained farther north in Tibet. While engaged in the recording of these profiles, they also installed stations in Nepal to record wide-angle reflections from the Moho beneath the Himalaya. These observations can be treated as three separate experiments. Four recordings made in the Arun Valley of Eastern Nepal at distances between about 190 and 250 km from the western shotpoint and three recordings near the Kathmandu Valley at distances of about 230, 260 and 305 km from the eastern shotpoint (figure 4) show strong signals that apparently are reflections from the Moho beneath the Greater Himalaya just west of Mount Everest (Lépine *et al.* 1984). Second, a series of recordings made in Nepal at somewhat different distances, of 100–150 km, and at different azimuths south of the western shotpoint reveal strong reflected phases with an apparent velocity of 7 km s^{-1} (figure 3 of Lépine *et al.* 1984). Finally a fan profile, extending southwards from one of those discussed above (figure 5), was constructed by using the middle shotpoint of the profile in southern Tibet and recorded by stations in southern Tibet and northern Nepal, across the Greater Himalaya (Hirn & Sapin 1984; Hirn *et al.* 1984*a*).

Some seismograms reveal more than one strong phase, suggesting a more complicated structure than simply an abrupt increase in velocity at the Moho. Among the four seismograms recorded in the Arun Valley from the western shotpoint, three recorded near one another at distances of about 230, 240 and 250 km show two coherent signals (figure 14). At each site, a clear signal arrives about 1.5 s earlier than would be predicted if the structure were the same as that determined for the region between the suture zone and the Greater Himalaya, and a second, sharper signal was recorded another 2 s earlier. The seismogram recorded in the Kathmandu Valley about 230 km from the middle shotpoint of the profile in southernmost Tibet also shows two phases (figure 14), with the later phase apparently arriving at the approximate time expected from a Moho transition centered at about 75 km depth, and with the second phase arriving 2 s earlier. Two more distant stations recorded only the earlier phase (figure 14), which Lépine *et al.* (1984) inferred to be a Moho reflection at a depth 15 km shallower than that beneath southern Tibet, or at a depth of 55 km (Hirn *et al.* 1984*a*). Lépine *et al.* (1984, p. 120) reported: 'Thus the Tibetan Moho is seen to extend at its 70–82 km depth as far south as the region of Mt. Everest.' With regard to the earlier reflected phase, attributed to a shallower Moho, they concluded: 'The depth of the Everest Moho is about 15 km less than the Tibetan Moho and it extends as far north as Mt. Everest.' Thus they envisage a step in the Moho somewhat north of Mount Everest.

Although the data probably are consistent with these conclusions, I am not convinced that these six seismograms with halfway points near the Greater Himalaya, can provide unique constraints on the dips and depths of the reflector. The existence of the later phase represents a complication, but inconsistencies in the presentation of the data make it very difficult to offer a concrete alternative to the interpretation given by Lépine *et al.* (1984). The broken lines that define arrival times of PmP (Moho) reflections north of the Himalaya and with which comparisons were made, are drawn differently on the two record sections (figure 14). The two seismograms recorded at 230 km from the two shots show travel times of the two later phases

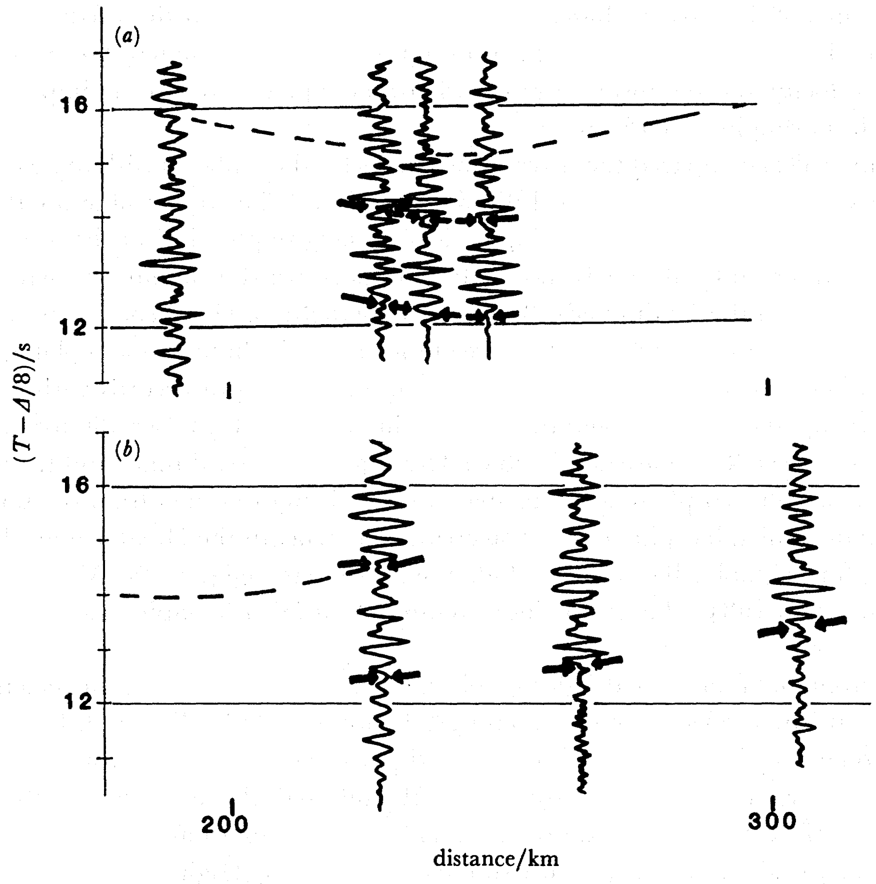

FIGURE 14. Seismograms showing wide-angle reflections, recorded in Nepal from explosions in southernmost Tibet (see figure 4). (*a*) Signals recorded in the Arun Valley from the Western shotpoint. Broken line shows observed arrival times for the east–west profile in southern Tibet, between the Indus–Tsangpo Suture Zone and the Greater Himalaya, where the crustal thickness is 70–75 km. The second strong phase arrives only 1 s earlier, suggesting that if the reflectors were flat, the one responsible for this phase would be nearly 70 km deep. The earlier arrivals presumably mark reflections from a shallower interface, at a depth of about 55 km (Hirn *et al.* 1984*a*). (*b*) Signals recorded near Kathmandu from the middle shotpoint on the profile in southern Tibet. Broken line is reportedly the same as in top figure. Note again the earlier arrivals that suggest a shallower reflector than that farther north. (From Lépine *et al.* 1984.)

that differ by about 0.5 s, but with one shown arriving at the predicted arrival time (figure 14*b*) and the other 1.5 s early (figure 14*a*). Thus, I cannot offer a simple explanation for the later phases that Lépine *et al.* (1984, p. 120) attributed to Moho reflections at '70–82 km depth as far south as the region of Mt. Everest', but I remain unpersuaded that they represent a continuation of an essentially flat Moho at a depth of 70 km as far south as the crest of the High Himalaya. Nevertheless, the relatively early signals almost surely represent reflections from depths many kilometres shallower than 70 km.

Lépine *et al.* (1984, figure 3) showed numerous seismograms recorded at distances of 120–150 km roughly south of the western shotpoint that show pairs of signals arriving with apparent velocities of about 7 km s^{-1}. On most seismograms, the earlier signal is the weaker and is followed about 1.3 s later by a stronger signal. Lépine *et al.* (1984) noted that both the strength and arrival times of the signals suggest that they are reflected phases from a major velocity contrast, such as the Moho. Assuming horizontal layers, they obtained a depth of about 35 km, for reflection points of the earlier phase, about 30 km south of the northern edge of the high peaks and near where the Main Central Thrust crops out. They also noted, however, that the high apparent velocity and the distance range where these phases are strong imply that they were reflected from dipping interfaces.

Hirn & Sapin (1984) compared the travel-time curves for these phases with those calculated for a structure with a shallow northward-dipping interface being responsible for the earlier reflected phase and a deeper southward-dipping Moho being responsible for the second phase. The shallower, intracrustal reflector is shown dipping northward at about 12°, with a depth of about 10 km beneath the Kathmandu Basin, extrapolated to 30 km beneath the shotpoint. The inferred dip of this surface is similar to those of the northerly dipping nodal planes of many fault-plane solutions of earthquakes in the Himalaya, and the depth accords with the depths of moderate earthquakes ($5.5 \leqslant$ magnitude $\leqslant 6.5$) in the Himalaya (see discussion above) (Baranowski *et al.* 1984; Ni & Barazangi 1984). Thus both the arrival times and the apparent velocity of this first reflected phase are consistent with its being reflected from the top surface of the Indian plate, which has plunged at a steeper angle beneath the Greater than the Lesser Himalaya (see, for example, Baranowski *et al.* 1984; Molnar 1984, 1988; Molnar & Chen 1982; Ni & Barazangi 1984). This is the interpretation that Hirn & Sapin (1984) give to this phase.

The greater strength of the second reflected phase implies a larger contrast in velocity at this reflector than at the first reflector. For reasons that do not seem to be discussed, Hirn & Sapin (1984) and Lépine *et al.* (1984) associate this second phase with reflections from a southward-dipping Moho. Thus, Lépine *et al.* (1984, p. 121) inferred the existence of three deep, essentially flat interfaces: one 'at 75 km beneath Tibet... as far south as the high Himalayas', 'a shallower one... at about 55 km', 'approximately between the High Himalayas and 50 km further south', and a third 'at a still shallower level, around 35 km... possibly downdipping towards south... on top of the Everest Moho'. Whereas the presentations given by Hirn & Sapin (1984) and Lépine *et al.* (1984), as well as a brief discussion by Pandey (1986) of reflected phases from an earthquake in Nepal and recorded there, show their data to be consistent with this structure, it seems to me that they have not eliminated the possibility that the Moho dips smoothly north.

Because of the similar apparent velocity and essentially constant delay of only 1.3 s between the earlier and later reflected phases with apparent velocities of 7 km s^{-1}, I find it easy to believe that the later phase is reflected from a surface parallel to, but deeper than, that causing the earlier phase. Recall that the Wind River Thrust Fault, in the western United States, was traced at depth by two strong signals about 1 s apart on a COCORP reflection profile (Smithson *et al.* 1979). I suspect that both phases observed by Hirn & Sapin (1984) and by Lépine *et al.* (1984) could be reflected from velocity contrasts within a thick, major fault zone between the Indian plate and the overlying Himalayan Thrust Sheet. If sedimentary rock from the Ganga Basin had been underthrust along this zone, as has been suggested (Acharya & Ray 1982; Lyon-Caen & Molnar 1983), then the fault zone could be associated with a thick zone of low-velocity material. It seems likely to me that the interfaces responsible for both phases with apparent velocities of 7 km s^{-1} dip north, and that the reflected phases responsible for at least one of the inferred steps in the Moho (Lépine *et al.* 1984) can be explained without a step.

The evidence most suggestive of southward-dipping interfaces beneath the Himalaya is from the fan profile constructed by using seismographs at distances of 170–305 km from the eastern shotpoint and recorded in southernmost Tibet and in Nepal (Hirn & Sapin 1984; Hirn *et al.* 1984*a*). These instruments were placed so as to record clear wide-angle reflections from depths of several tens of kilometres, and in particular from the Moho. In presenting the data, Hirn & Sapin (1984; Hirn *et al.* 1984*a*) corrected the arrival times for the different distances (between 170 and 305 km) at which the recordings were made so that reflections from horizontal interfaces at the same depths of 50–70 km would be aligned. They then plotted the seismograms so that the time axis is translated into depth in kilometres (figure 15). Although this has the effect of vividly portraying the seismograms in a physically interpretable manner, the absence of specific information about arrival times at different stations, the locations of the stations, and the timescale in seconds render any further quantitative analysis by the reader difficult.

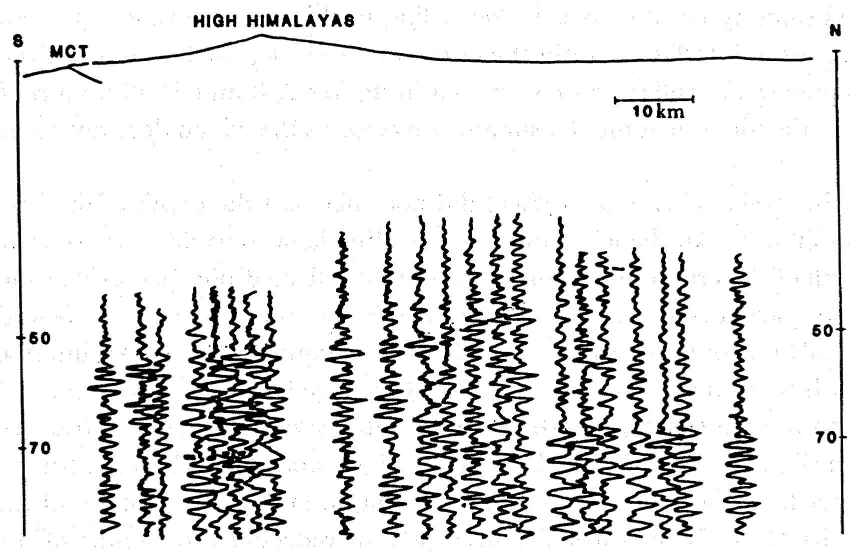

FIGURE 15. Wide-angle reflections recorded on a north–south profile across the Greater Himalaya, from Nepal to Tibet, as distances of 170–305 km from the middle shotpoint along the southern refraction profile (see figure 4). Arrival times have been adjusted for different recording distances and plotted to illustrate probable depths of reflectors. Coherent reflections from about 70 km on the right (north) and from about 55 km on the left (south) are clear. Note the possible northward continuity of the shallower reflector to shallower depths, marked by strong signals corresponding to depths of 55–45 km on the middle traces. Note also strong signals that follow these signals, corresponding to depths of 62 km on the 9th and 10th traces from the left, of 65 km, 69 km, and 72 km on the 11th, 12th, and 13th traces, and of 75 km on the 14th and 15th traces from the left. I suspect that these signals might be reflections from a northward-dipping Moho. (Modified from Hirn & Sapin 1984.)

The coherency of signals recorded north and south of the Greater Himalaya are consistent with their being reflections from a strong continuous reflector, such as the Moho. As noted above, the first strong signal from the eastern shotpoint and recorded at stations tens of kilometres north of the Greater Himalaya corresponds to a reflection from about 70 km (seven traces on the right in figure 15). The arrival times of the first strong signals recorded from stations south of the Greater Himalaya are appropriate for reflections at depths of 50–55 km (eight traces on the left of figure 15). As plotted, the arrival times, adjusted for different distances, suggest a slight southward dip of this interface, but this effect probably could be caused by differences in corrections for distance and by lateral variations in the local velocity structure.

Between these groups of recording sites, the arrival times of the first strong phase at the more northerly sites suggest a shallower depth of this reflector; the apparent depth of about 50 km beneath the crest of the Greater Himalaya decreases to 45 km some 30 km farther north (figure 15). These phases can be seen clearly; they are the strongest signals on three of seven traces (the 9th, 11th and 15th traces from the left in figure 15). Stronger signals are recorded later on the 10th, 12th, 13th and 14th traces from the left in figure 15, but on the 10th, 13th and 14th traces, signals can be observed at the times corresponding to depths of about 55, 45 and 45 km, respectively.

Hirn & Sapin (1984; Hirn *et al.* 1984*a*) did not give sufficient information for me to be convinced that these arrivals represent an interface dipping south or to show that such an interface is the Moho. Note that on the basis of both their observed and their calculated seismograms (figure 2 of Hirn *et al.* 1984*a*), reflections from a Moho at a depth of 70 km might be too weak to be recorded at distances less than 200 km, and perhaps the absence of reflections from 70 km on some traces is caused by recording in this distance range. Moreover, because reflected phases from interfaces within the crust can be strong, such as some of those shown in figure 3 of Lépine *et al.* (1984) or those shown in figures 2, 3 and 4 of Sapin *et al.* (1985) for southern Tibet, the identification of a shallow reflector as the Moho does not seem required to me.

Hirn & Sapin (1984; Hirn *et al.* 1984*a*) did not infer that the depth of the Moho increases smoothly from 50 or 55 km beneath the Greater Himalaya to as deep as 70 or 75 km tens of kilometres north of the crest of the range, and indeed reflected phases marking such a dipping interface are not particularly well defined on the seismograms in figure 15. Nevertheless, there are strong signals on some traces that could be reflections from such an interface. A strong signal on the 9th trace and the strongest on the 10th trace from the left in figure 15 are plotted as if reflected from about 62 km depth. A complicated signal on the 11th trace could mark a reflection from slightly a greater depth (64 km). Signals on the 12th and 13th traces, both of which are larger than those presumed by Hirn & Sapin (1984) to mark a southward dipping Moho at depths of 45–55 km, would correspond to reflections at depths of about 69 and 72 km, respectively. Finally, signals can be seen on the 14th and 15th traces at times corresponding to depths of about 75 km. These signals are not as coherent on neighbouring traces as those arriving earlier and interpreted by Hirn & Sapin (1984; Hirn *et al.* 1984*a*) as reflected from a shallow south-dipping interface. Nevertheless, the existence of these phases suggests to me that these authors have not eliminated the possibility that the Moho does dip smoothly beneath the Himalaya, but that it is masked somewhat by complexity in the crust at shallower depths, and by the effects of recording these signals at different distances.

In reviewing the seismic refraction studies of the Himalaya, I have taken a prejudiced view. With no preconceived notions of what Hirn and his colleagues should have found, much of the structure that they inferred is as reasonable as any. Accordingly, I certainly cannot assert that they are wrong in what they deduced. At the same time I feel strongly that the brevity of the data presentation allows one the freedom to doubt their interpretations. Specifically, I do not think that they have eliminated the possibility that the Moho does dip smoothly to the north beneath the range. First, I think that the pair of phases with apparent velocities of 7 km s^{-1} (figure 3 of Lépine *et al.* 1984), which comprise some of the evidence for one of their inferred steps in the Moho, can be interpreted as reflections from the northward dipping, top surface of the Indian plate plunging beneath the Himalaya. Second, I can see a hint of a northward-dipping reflector between depths of 50 and 70 km on traces 9–15 in figure 15, which could mark a smoothly northward-dipping Moho. Thus I proceed with the assumption that the Moho beneath the Himalaya is not sliced by southward-dipping faults, but is a continuous, smooth, northward-dipping surface.

Gravity anomalies across the Himalaya

Gravity anomalies lack the resolution to define details of deep crustal structure, and because of their inherent non-uniqueness, they are best used to answer more specific questions than 'What is the deep structure?' They can be much more effectively used to disprove, than to prove, particular hypothesized structures. At the same time, gravity anomalies, unlike other observable quantities, are directly sensitive to mass distributions, and because the force of gravity acting on lateral variations in density is the ultimate force that drives most tectonic processes, gravity anomalies can provide direct constraints on such processes. My review will focus more on this aspect of gravity anomalies than on their use solely as a constraint on hypothetical density structures.

Gravity measurements are most easily compared with calculations by reducing them to the values that would be measured at a common altitude, usually sea level, either to free air or to Bouguer anomalies. Terrane corrections are commonly added to Bouguer anomalies, but rarely, if ever, to free-air anomalies. One difficulty in using gravity anomalies from the Himalaya is that terrain corrections can be enormous (up to 100 mGal) and cannot be ignored. Therefore, one must consider Bouguer anomalies.

Because of the great height of the Himalaya and because of approximate, but incomplete, isostatic equilibrium, the crust beneath the Greater Himalaya is thicker than that of the Lesser Himalaya. Consequently, Bouguer anomalies decrease northward with increasing elevation, and their negative values become large over the Greater Himalaya (Choudhury 1975; Das *et al.* 1979; Duroy *et al.* 1987; Kono 1974; Marussi 1964; Mishra 1982; Qureshy 1969; Qureshy & Warsi 1980; Qureshy *et al.* 1974; Teng *et al.* 1980; Warsi & Molnar 1977). This northward decrease in Bouguer anomalies is characteristic of the Himalaya, and in early studies of gravity it was used as an argument in support of the concept of isostasy. Now, with more and better data, the subtleties in the northward gravity gradient, rather than its mere existence, are the focus of most modern analyses. The easiest way to appreciate the significance of a profile of gravity anomalies is compare it with a reference; in this case the best reference, or the simplest model, is that of local Airy-type isostatic equilibrium.

Deviations from local isostatic equilibrium

For local Airy isostatic equilibrium, the thickness of the crustal root should be proportional to the elevation. To examine whether the Himalaya are in local isostatic equilibrium, Lyon-Caen & Molnar (1985) compared measured Bouguer anomalies with those calculated from the corresponding average topographic profiles, assuming local isostatic equilibrium (figure 16). Systematic deviations from isostatic equilibrium can be seen for each of the five profiles considered. Observed gravity anomalies over the Indo-Gangetic Plain are as much as 100 mGal more negative than those calculated. Thus a large mass deficit must be present beneath the flat plain. Over the transition from the Lesser to the Greater Himalaya, observed anomalies are as much as 100 mGal less negative than those calculated (see also Tang *et al.* 1981). Thus, a mass excess (with respect to local isostatic equilibrium) must underlie this segment of the

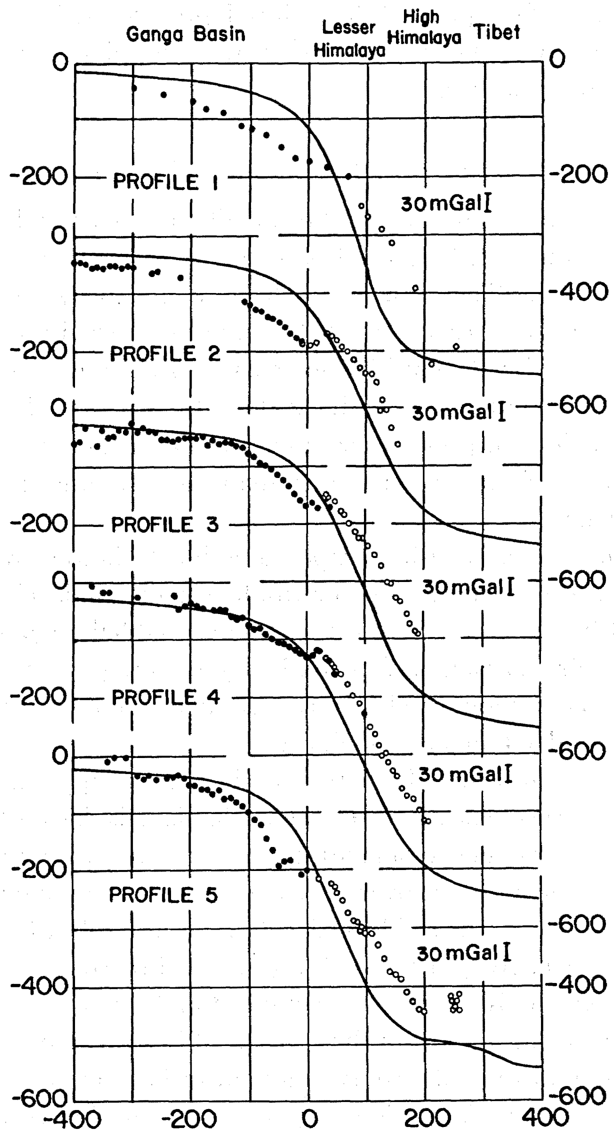

FIGURE 16. Bouguer gravity anomalies for five profiles shown on the map in figure 4. The edge of the Ganga Basin next to the Lesser Himalaya defines the origin, $x = 0$. Solid curves show calculated Bouguer gravity anomalies for structures in isostatic equilibrium with the topographic profiles. Note the poor fit in all cases, with calculated anomalies too small over the Ganga Basin and too large over the Lesser Himalaya. Thus, a mass deficit underlies the basin, and a mass excess underlies the mountains. (From Lyon-Caen & Molnar 1985.)

range. The Himalaya and the neighbouring Indo–Gangetic Plain clearly are markedly out of local isostatic equilibrium.

The reason for examining whether or not the Himalaya is in local isostatic equilibrium is not so much to test that idea but more to gain insight into how deviations from isostatic equilibrium might occur. The well-known existence of a basin beneath the Indo–Gangetic Plains, the Ganga Basin, which is filled with several kilometres of late-Cainozoic sedimentary rock (Karunakaran & Ranga Rao 1979; Lillie & Yousuf 1986; Raiverman *et al.* 1983; Sastri *et al.* 1971), offers an explanation for where at least some of the mass deficit lies. Correspondingly, some authors have postulated the existence of dense rock within the crust of the Lesser

Himalaya to explain the more positive observed anomaly than would be predicted from local isostatic equilibrium (see, for example, Qureshy 1969; Qureshy *et al.* 1974). Gravity anomalies alone, however, can neither prove nor disprove such hypothetical density distributions, and thus to gain insight into the significance of the deviations from local isostatic equilibrium, one must look beyond density as a physical parameter to be adjusted in calculations.

Because deviations from isostasy imply deficits and excesses of mass in the crust and/or mantle, and because such deficits and excesses must be supported by stress differences within the crust and mantle, deviations from isostatic equilibrium can place bounds on the strength of the crust and mantle (see, for example, McKenzie 1967). In the limiting case of a very strong lithosphere, such as on the Moon or Mars, large deficits and excesses of mass, and hence large variations in density, can be supported and maintained for long periods of time. In the other limit of a very weak lithosphere, the buoyancy associated with mass deficits would cause them to rise, and mass excesses would sink, until isostatic equilibrium prevailed. When viewed in this context, the simplest questions to be asked address the 'strength' of the lithosphere, or more precisely, its flexural rigidity. A plate with a large flexural rigidity can support heavy localized masses with only a small deflection, but one with a small flexural rigidity will bend substantially, so as to allow the mass anomalies to be nearly in isostatic equilibrium (Turcotte & Schubert 1982, pp. 104–133). Thus most modern analyses of gravity anomalies over regions with dimensions of hundreds of kilometres pay little attention to the distribution of density within the crust; instead they consider the implications of the gravity anomalies for the physical mechanisms that support various possible distributions of density that, in turn, are allowed by the gravity measurements.

In the context of the Himalaya and the Indo-Gangetic Plains, the lithosphere seems to be flexed down beneath the plains, which are filled with sediment, but the strength of the plate supports a heavy load over the Lesser Himalaya. The abundant evidence for thrust faulting within the Himalaya implies that slices of crust have been thrust southwards onto intact Indian crust. Thus the load consists of those slices. In addition, the sequence of ages and sedimentary facies of the Siwalik sequence, which fills the Ganga Basin, imply both a tilting and a subsidence of the Ganga Basin consistent with its being underthrust beneath the Himalaya (Lyon-Caen & Molnar 1985). Thus the mass deficit beneath the Indo-Gangetic Plain, inferred from the deviation from isostatic equilibrium, probably exists because the Indian plate is flexed down, and the excess mass over the Lesser Himalaya would be part of the mass of the load that flexes the plate down. The strength of the plate contributes to the support of that excess mass.

Flexure of a simple elastic plate

The simplest mechanical model commonly used to quantify the flexure of the lithosphere is an elastic plate overlying an inviscid fluid and loaded by masses above, within, and below the plate. Such a model is an obvious oversimplification both because the lithosphere probably does not deform as an elastic plate and because it is underlain by material with finite viscosity. Moreover, although this simple model is quite effective for some situations, it clearly fails in others, so that some workers have replaced it with viscoelastic plates, elastic-perfectly plastic plates with finite yield stresses, plates with creep-strength profiles based on laboratory measurements of flow laws of the constituent minerals, and others. All such models also are approximations, especially given that stresses created by the flow of material at the base of the lithosphere and within the asthenosphere are likely both to warp the overlying plate and to support lateral variations in density. Thus in my view, the value of all of these models is revealed less by their ability to offer simple physical explanations for some observations than by the understanding of how the flexure of such plates fails to account for all of these data.

As of 1987, analyses of gravity anomalies over the Himalaya have considered only elastic plates. The first step in such analyses was to consider a semi-infinite elastic plate with a constant flexural rigidity beneath the Central Indian Highlands, the Indo–Gangetic Plain, and the Himalaya (Duroy *et al.* 1988; Karner & Watts 1983; Lyon-Caen & Molnar 1983, 1985). With such a simple model (figure 17), six parameters are left free to be adjusted: the flexural rigidity

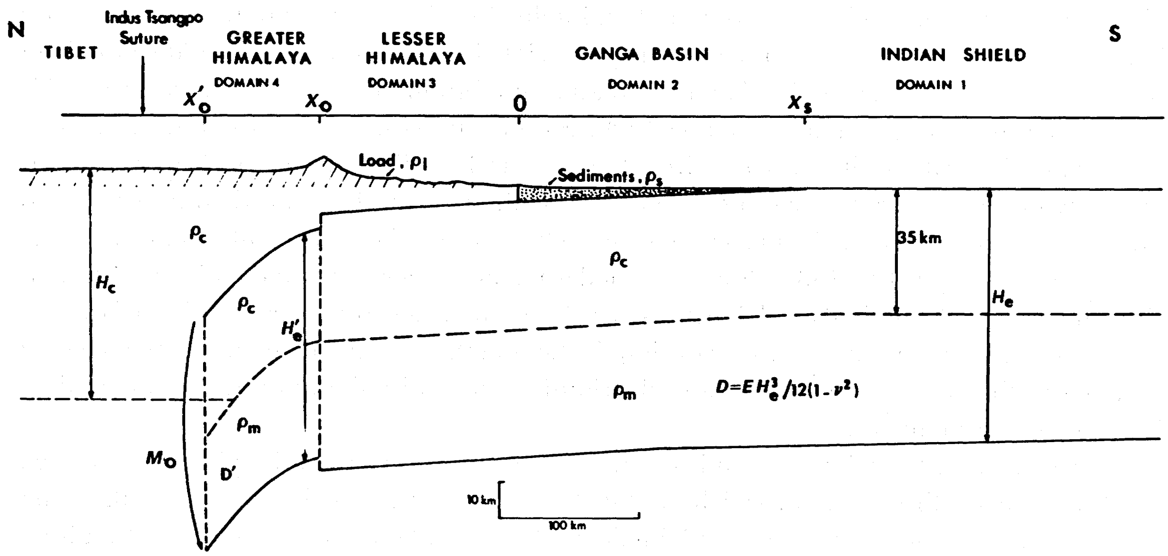

FIGURE 17. Simple plate model used to examine the gravity anomalies. An elastic plate underlies the Indian Shield, the Ganga Basin, and the Himalaya and is loaded by the weight of the Himalaya. The initial analysis by Lyon-Caen & Molnar (1983) examined a plate of constant flexural rigidity, D, and extending to the coordinate X_0. Later analyses considered a segment with a lower flexural rigidity, D', attached at X'_0. Final analyses included the effects of a bending moment and a vertical force (per unit length) acting at the end of the plate. (From Lyon-Caen & Molnar 1983.)

of the plate, the coordinate of the end of the plate (X_0), the force per unit length (F_0) and the bending moment per unit length (M_0) applied to the end of the plate, and the two independent density differences among the three relevant densities: mantle, crust and sedimentary fill in the Ganga Basin. (Note that Karner & Watts ignored the density difference between crust and sedimentary fill and assumed the same average value for both the sediment and the overthrust mass comprising the Himalaya, and that Duroy *et al.* specified numerous different densities for different units in the foreland basin of Pakistan.) Initially, calculations were made ignoring the force and the bending moment at the end of the plate. For the cases where the end of the plate was taken to lie south of the Indus–Tsangpo Suture Zone, Lyon-Caen & Molnar (1983) assumed that the depth of the Moho increased linearly from its calculated depth at its northern end to a depth of 65 km beneath southern Tibet, where local isostatic equilibrium was assumed to exist. Lyon-Caen & Molnar (1983) then performed numerical experiments to examine the sensitivity of calculated gravity anomalies to those four remaining parameters: flexural rigidity, position of the end of the plate, and the two density differences.

Variations among reasonable density differences were found to have little effect on calculated gravity anomalies. For example, if the assumed density of the sediment in the Ganga Basin were increased, the calculated deflection of the plate also increased so that the increased gravitational attraction of the more dense sediment was compensated by its increased thickness and the decreasing amount of underlying mantle.

The effect of varying the flexural rigidity of the plate was most clearly seen in the calculated gravity anomalies over the Indo–Gangetic Plain and the Lesser Himalaya. Tight constraints could not be placed on its value, and the uncertainty in the flexural rigidity is at least a factor of three for each profile. Moreover, flexural rigidities deduced for different profiles across the Himalaya differ by at least three times, and possibly by 10 times or more (Duroy *et al.* 1987; Lyon-Caen & Molnar 1985). The large uncertainties in all estimates makes it impossible to map variations in flexural rigidity precisely, but clearly a variation of three times inferred for profiles only 200 km apart calls for caution in interpreting the inferred values, as well as in trusting too much the simple model of an elastic plate. In any case, the inferred flexural rigidities are much larger (10–1000 times) than those deduced for the Alps (Karner & Watts 1983) or the Apennines (Royden & Karner 1984), or the transverse ranges of California (Sheffels & McNutt 1986).

The parameter that affects the calculated gravity anomalies most and that also is most difficult to interpret is the position of the end of the plate. Ignoring any force applied to the end of the plate, the load that flexes the plate down was taken to be the weight of the portion of the Himalaya that overlies the plate. Thus, in Lyon-Caen & Molnar's (1983) calculations, only the portion of the Himalaya that directly overlies the plate is supported by it. The support of the Himalaya between the end of the plate and southern Tibet was, initially, ignored. The farther north that the plate is assumed to extend beneath the Himalaya, the greater is the assumed load on it, and the greater is the calculated deflection of the plate (figure 18). If only the southernmost hundred kilometres of the Lesser Himalaya comprised the load, this load would be insufficient to flex the plate down enough to create a basin as deep as the Ganga Basin; calculated gravity anomalies are too small. In the case where the elastic plate extends beneath 250 km of the Himalaya to the Indus–Tsangpo Suture Zone, the weight is so large that the calculated depth of the Ganga Basin is too large, and the calculated gravity anomalies are much too negative. Thus, Lyon-Caen & Molnar (1983, 1985) concluded that the loading and flexing of an elastic plate of constant flexural rigidity cannot account for the gravity anomalies across the entire Himalaya or for how the range is supported. Accounting for both the gravity anomalies and the support of the range, therefore, requires a more complicated mechanical model.

Elastic plate with a variable flexural rigidity

The gradient in the Bouguer gravity anomalies steepens markedly over the Himalaya, with gradients of less than 1 mGal km^{-1} across the Indo–Gangetic Plain and as much as 2 mGal km^{-1} across the Greater Himalaya (figure 16). This steepening of the gradient is most simply explained by a steepening of the Moho, from a dip of only 2–4° beneath the Indo–Gangetic Plains to a dip of 10–20° beneath the Greater Himalaya (Choudhury 1975; Das *et al.* 1979; Kono 1974; Lyon-Caen & Molnar 1983, 1985; Mishra 1982; Teng *et al.* 1980; Warsi & Molnar 1977).

Clearly, other distributions of density could explain the gravity gradient, but an increase in

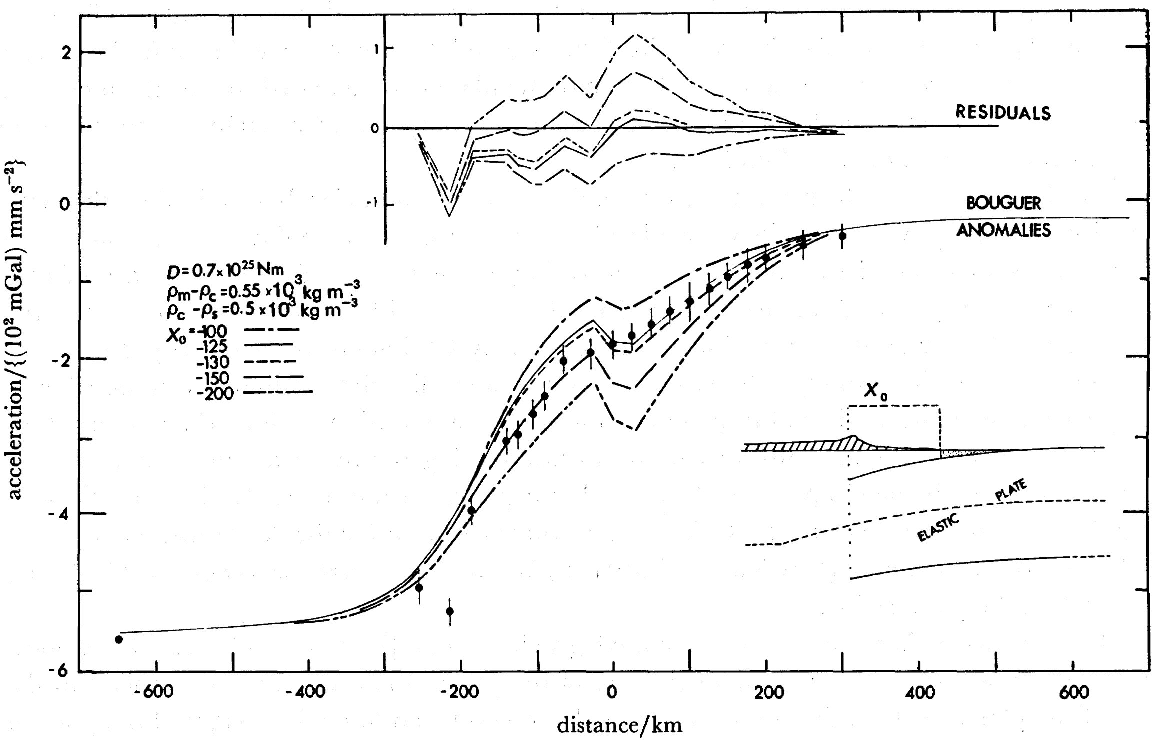

FIGURE 18. Comparisons of measured Bouguer anomalies along the easternmost profile in figure 4 with calculated anomalies for plates extending different distances beneath the Himalaya. Only the material between the Ganga Basin and X_0 comprises this load. In these calculations, the Moho north of X_0 was drawn as a northward-dipping plane to $x = 250$ km, where isostatic equilibrium is presumed to prevail and where the depth of the Moho below sea level was taken to be 65 km. Note the excessively large calculated gravity anomalies for $X_0 = 150$ km, because the load is too heavy and the plate is flexed too much, and the small values for $X_0 = 100$ km, for which the load of the Himalaya is too small. (From Lyon-Caen & Molnar 1983.)

the average depth of the Moho is also required by Hirn *et al.*'s (1984*a*, Hirn & Sapin 1984) demonstration that the Moho is at a depth of 70–75 km north of the Greater Himalaya and at shallower depths farther south. For a depth of 43 km at the foot of the Himalaya (38 km of typical crust of the Indian Shield (Kaila 1982) plus 5 km of Siwalik sedimentary rock (Karunakaran & Ranga Rao 1979; Raiverman *et al.* 1983; Sastri *et al.* 1971)) and for 70 km below the area 150 km further north, the average dip of the Moho beneath the Lesser and Greater Himalaya is 10°. Obviously, if the average dip of the Moho is gentler beneath the Lesser Himalaya, it must be steeper beneath the Greater Himalaya. Thus, in so far as the Moho is a relatively smooth surface beneath the Himalaya, a steepening of it beneath the Greater Himalaya seems to be required.

The following discussion proceeds from the supposition that the Moho is a smooth surface and is not cut by southward dipping faults as inferred by Hirn *et al.* (1984*a*; Hirn & Sapin 1984). Gravity anomalies, however, cannot prove that the Moho is smooth; in fact, Hirn & Sapin (1984) demonstrated that their inferred structure with steps in the Moho is consistent with observed gravity measurements in the Himalaya. If their inferred structure is shown to be correct, most of the following discussion of gravity anomalies will be rendered worthless.

The steepening of the Moho from *ca.* 3° to *ca.* 15° in a distance of approximately 100 km implies that in cross section the average radius of curvature of the Moho is about 150–200 km, and therefore that the Indian plate is much more severely bent beneath the Himalaya than it is beneath the Indo–Gangetic Plain. For the plate to bend sharply beneath the range, its flexural rigidity there must be much less than that beneath the plains.

Recognizing this, Lyon-Caen & Molnar (1983) calculated gravity anomalies across the Himalaya by using a simple model of an elastic plate with a northward decrease in the flexural rigidity. This was implemented by treating the Indian plate as a semi-infinite plate with a constant flexural ridigity beneath the Indo–Gangetic Plains and the Lesser Himalaya and with a short segment of plate with much lower flexural rigidity attached to it and underlying the Greater Himalaya. This model contains eight free parameters: the same two density differences as before, two flexural rigidities, the position where the two plates are joined, the position of the end of the plate, and the force and moment at the end of the plate. Initially the force and the moment were ignored. Calculations show that the addition of a segment of plate with a small flexural rigidity yields steep dips of the Moho and steep gravity gradients beneath the Greater Himalaya (figure 19). As with a single plate of constant flexural rigidity, however, the weight of the Greater Himalaya is so large that in all calculations, it causes a very large downward bending of the plate, and calculated gravity anomalies over the Lesser Himalaya and the Ganga Basin are significantly more negative than observed. Thus some additional force must contribute to the support of the Himalaya; in the absence of that force, the entire Himalayan Range would be lower than it is by a couple of kilometres, the Ganga Basin would be deeper by one or two kilometres, and the Moho beneath both would likewise be deeper.

Additional forces acting on the Indian plate

It might be tempting to infer that thermal expansion of material in a hot upper mantle beneath the Himalaya has caused the surface of the range to stand higher than it would if the underlying mantle were cold. Although one cannot rule this possibility out on a local scale, the mantle beneath the Indo–Gangetic Plains and Lesser Himalaya is not likely to be hot. The seismic observations discussed above seem to rule that out. Moreover, were it hot, although the low density of the hot upper mantle would buoy up the crust and make the Moho shallower than normal, it would also contribute compensating negative gravity anomalies.

A sufficiently large bending moment applied to the end of the plate can flex the plate up beneath both the Lesser Himalaya and the Indo–Gangetic Plains and down beneath the Greater Himalaya. Thus its inclusion in the calculations can contribute to the support of the range as well as cause a steepening of the Moho, and hence of the Bouguer anomaly gradient, beneath the Greater Himalaya. A large range of possible values for the bending moment can be found for an allowable range of possible flexural rigidities of the short segment of plate beneath the Greater Himalaya (Lyon-Caen & Molnar 1983). Consequently, useful constraints cannot be placed on the value of such a bending moment (per unit length) except that it must be at least 5×10^{17} N (figure 20).

Two possibilities for the origin of a bending moment suggest themselves: a horizontal force (per unit length) acting on a deflected plate and a vertical force (per unit length) acting on a cantilever attached to the end of the plate. The horizontal force is not a likely source. For a plate deflected $y_0 = 30$ km, the horizontal force per unit length, $F_0 = 2\,M/y_0$, necessary to create a moment per unit length of $M = 5 \times 10^{17}$ N, must be at least 3.3×10^{13} N m^{-1}. For a plate 100 km thick, this would correspond to an excess horizontal compressive stress of at least 330 MPa (or 3.3 kbar). Such a large regional horizontal compressive stress seems unlikely.

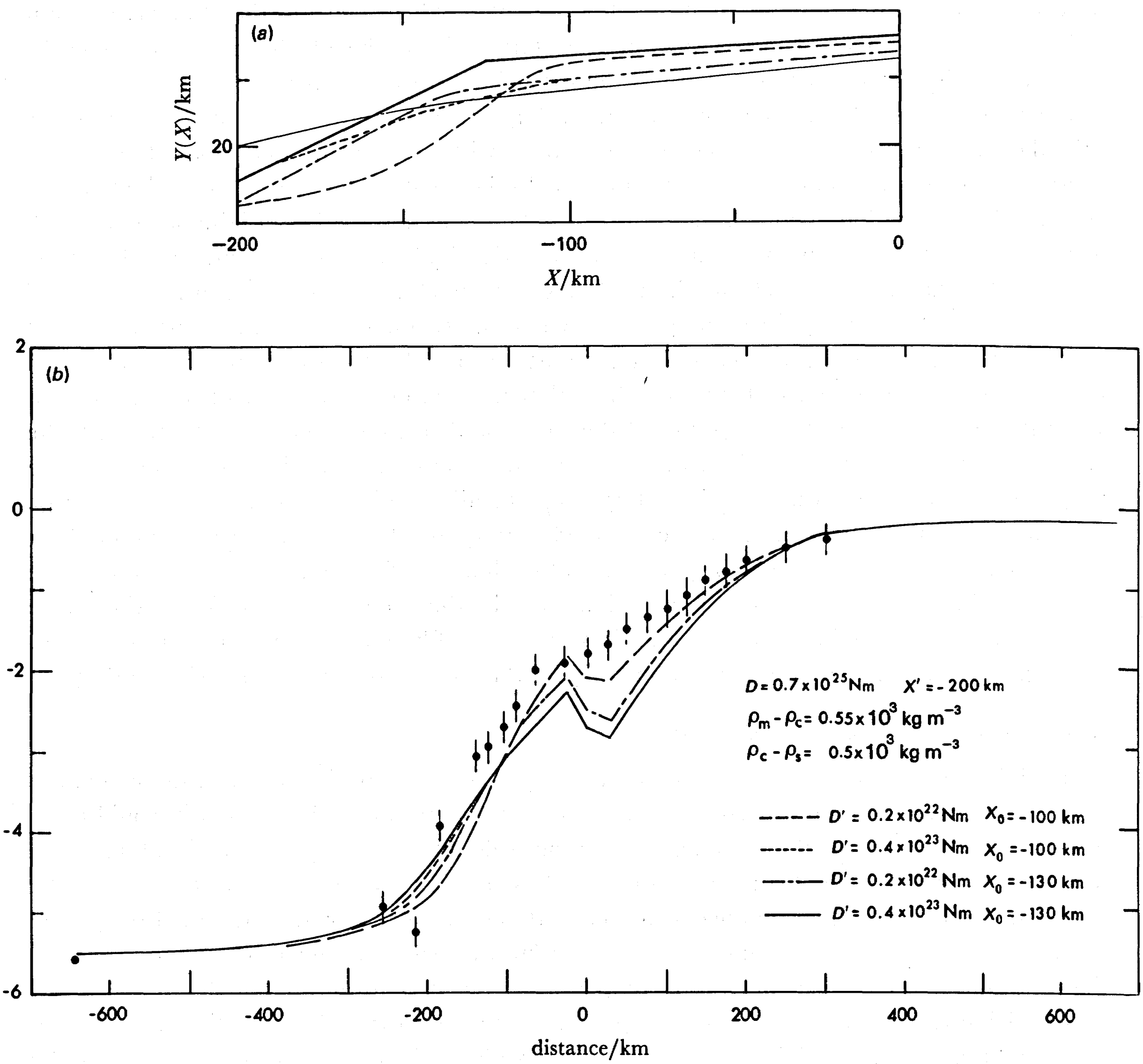

FIGURE 19. Deflections of the Indian plate (*a*) and Bouguer gravity anomalies (*b*) assuming the two plate model in figure 21. (*a*) Dark solid line shows the cross-sectional shape of the Moho that yields a good fit to gravity anomalies, and other lines show calculated cross-sectional shapes for different flexural rigidities (D') of the short segment of plate and different positions (X_0') where it is joined to the semi-infinite plate. (*b*) Calculated gravity anomalies are shown for the same parameters (listed on the figure) used in calculating the deflections. Note poor fits in all cases. The weight of the Himalaya is so large that calculated deflections of the plate are too large to yield a match to the observed gravity anomalies. Thus the weight of the Himalaya is too large to be supported by any combination of elastic plates without some additional force acting on the plate. (From Lyon-Caen & Molnar 1983.)

If the crust (or part of it) were scraped off the underthrusted continental lithosphere, then gravity acting on the mantle lithosphere, particularly if the lower crust attached to it underwent a phase change to eclogite facies (Richardson & England 1979), could contribute a substantial vertical force per unit length. The force (per unit length) acting on a slab of lithosphere more dense than the asthenosphere by $\delta\rho = 50\ \mathrm{kg\ m^{-3}}$ (*ca.* 500 K colder than surrounding asthenosphere) and with a thickness of 50 km and a length of 200 km would be

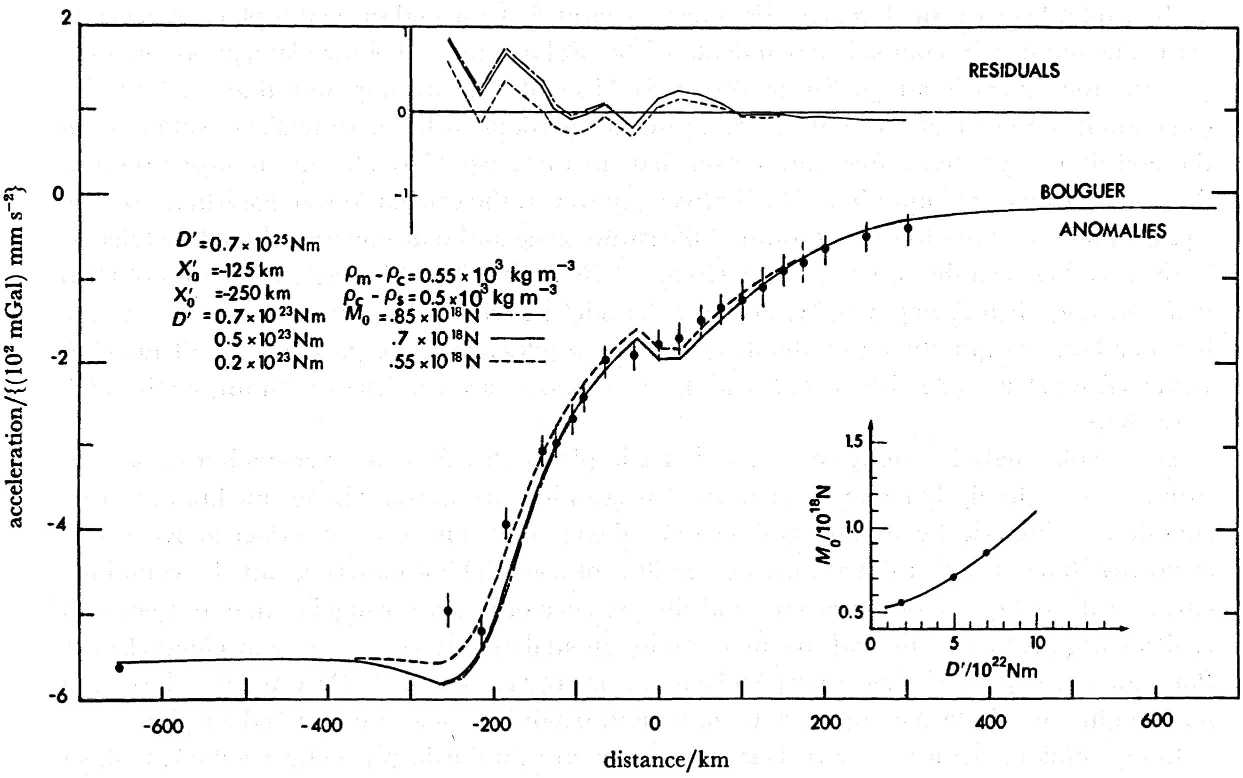

FIGURE 20. Comparison of calculated and observed Bouguer anomalies for models (figure 17) with two segments of plate with different flexural rigidities and with bending movements applied to the end of the plate. Plot in lower right shows the trade-off between values of D' and the bending moment. Note the wide range of values for both parameters and the clear impossibility of resolving their values with additional, or better, measurements of gravity. (From Lyon-Caen & Molnar 1983.)

PHILOSOPHICAL TRANSACTIONS OF THE ROYAL SOCIETY A MATHEMATICAL, PHYSICAL & ENGINEERING SCIENCES

5×10^{12} N m^{-1}. If centred 100 km from the end of the elastic plate, the bending moment would be 5×10^{17} N. Thus, gravity acting on a slab of mantle lithosphere with crust either detached from it or having undergone a phase change to a more dense mineralogy could cause the necessary bending moment.

Proving such a simple explanation is virtually impossible, at least at present. Lyon-Caen & Molnar (1983, 1985) were content with finding one set of reasonable parameters that allow a fit of observed and calculated gravity anomalies and depths to the basement of the Ganga Basin. The trade-offs among flexural rigidities, positions of the ends of the plates, and values of the forces and bending moments make deducing a unique, or even well constrained, set of parameters impossible. Moreover, because the postulated cold mass that would cause the bending moment should lie 100 km or more north of the suture zone, direct evidence, either with gravity anomalies or with seismic wave propagation, for its existence or absence does not yet exist. The evidence most suggestive of cold material north of the Himalaya is from the Karakoram region, discussed below, but it too is inconclusive.

The analysis of a flexed plate loaded by a force and a bending moment on its end led to one prediction that, if taken literally, appears absurd but might nevertheless be qualitatively observable in the seismic and gravity data. In all Lyon-Caen & Molnar's calculations, the flexed plate is taken to include a section of crust with constant thickness, and the steep gradient of the Moho beneath the Greater Himalaya requires that the end of such a plate be severely bent. The result is that our calculated depth of the Moho at the end of the plate, approximately beneath the Indus–Tsangpo Suture Zone, is 115 km! The assumptions that lead to this calculation are not realistic, but adjusting the calculations to be more realistic would entail the addition of yet more free parameters that, in turn, would render the interpretation of the other parameters impossible. Qualitatively, however, the calculations suggest that isostatic equilibrium ought not to prevail south of the suture zone and that the crust should be thickest in the area between the suture and the Greater Himalaya. The wide-angle reflections of Hirn *et al.* (1984*a*; Hirn & Sapin 1984) do show the thickest crust in that area (figure 5), and the hint of a Bouguer gravity low of about 30 mGal in profiles across this part of Tibet (Tang *et al.* 1981; Wang *et al.* 1982; Zhou *et al.* 1981), noted above, are consistent with unusually thick crust there.

The whole analysis strictly in terms of elastic plates clearly is an oversimplification and, surely at some level, dynamically supported stresses in a deforming viscous medium must be considered. Numerical experiments show that when a fluid convects, the surface above a zone of downwelling is pulled downward by the flow of cold sinking material, but the combined effects of the deflection of the surface and the presence of heavy downgoing material beneath it yields negative (isostatic and free-air) gravity anomalies over zones of downwelling (Lin & Parmentier 1985; McKenzie 1977; McKenzie *et al.* 1974; Parsons & Daly 1983). Thus, such flow might contribute the appropriate forces and bending moment to the Indian plate.

In my opinion, further analysis of elastic-plate models for the deep structure of the Himalaya is not likely to yield important constraints on the structure or on the dynamics of mountain building. Although the model of an elastic plate beneath the Indo–Gangetic Plains and the Lesser Himalaya accounts for the deep structure of these regions, surely other models, with more realistic rheologies, will also do so. To explain the gravity anomalies beneath the Greater Himalaya in terms of a flexed plate, the flexural rigidity must be considerably smaller in that area than beneath the Lesser Himalaya and farther south. Moreover, an elastic-plate model is unable to account for the support of the high range of mountains without an additional force being applied to the plate. Thus, in my opinion, to match the gravity anomalies with a structure satisfying mechanical equilibrium of a simple flexed elastic plate requires a knowledge of too many independent parameters; the trade-offs among them, especially given the mechanical oversimplification of a purely elastic plate, make the introduction of additional complexity, describable by additional parameters, unlikely to allow additional understanding without independent constraints on some of the parameters.

The value of the simple model of an elastic plate, like most simple physical models, lies as much in the aspects in which it fails as in those in which it succeeds. In this context, the recognition of the need for an additional force acting on the Indian plate and contributing to the support of the Himalaya is the most important implication.

Deep structure of the Karakoram

The Karakoram Range lies at the narrow western end of the Tibetan Plateau, midway between the Indian Craton on the south and Tarim Basin on the north (figures 1 and 4). The Indian subcontinent is actively underthrusting the Himalaya, and the Tarim Basin has been (and probably continues to be) underthrust southward beneath the western Kunlun, the range on the northern edge of the plateau. Thus in the area of the Karakoram, crustal shortening occurs both north and south of the range and one might expect the convergence of the subcrustal portions of lithosphere to manifest itself as measurable geophysical anomalies. Because there is some evidence suggesting that the upper mantle is unusual beneath the Karakoram, I isolate this area from the discussions of Tibet and the Himalaya, given above, and describe these features.

Gravity anomalies across the Karakoram

As part of the Sino–Swedish expeditions in the 1920s and 1930s, Amboldt (1948) measured gravity at a number of sites in the Karakoram, Kunlun and Tarim Basin. At present, his measurements are the only published ones north of the Karakoram. Later Marussi (1964) reanalysed the measurements, added terrain corrections, and also computed isostatic anomalies, for various assumed reference crustal thicknesses. He found the pattern described above for the Himalaya to be mirrored on the northern edge of Tibet: a negative isostatic anomaly marked the southern edge of the Tarim Basin and a positive isostatic anomaly characterized the northern edge of the Kunlun.

This pattern of mass deficit over a foreland basin and mass excess over the neighbouring range is reminiscent of the Himalaya (discussed above) and other ranges. Thus, aware that Norin (1946) had mapped folded Tertiary rock, overthrust by Cretaceous rock on the northern margin of the Kunlun, Lyon-Caen & Molnar (1984) pursued an analysis of the gravity anomalies in terms of the simple model of a semi-infinite elastic plate over an inviscid fluid, loaded solely by the weight of the range above the plate. To match the gravity anomalies with such a model, the plate must extend 80 km southward beneath the Kunlun Range, and probably 100 km or more. No upper limit could be placed on the southward extent of such a plate. Taken literally, this suggests a comparable amount of underthrusting, of at least 80 km, of the Tarim Basin beneath the Kunlun. Both because Amboldt's (1948) measurements of gravity and elevation are relatively inaccurate, and because the elastic plate model is an oversimplification, however, it probably is wiser merely to conclude that underthrusting of the Tarim Basin of some tens of kilometres (or more) has occurred.

Not only do the gravity anomalies on and adjacent to the ranges north and south of the Karakoram indicate marked deviations from local isostatic equilibrium, but so do those from the Karakoram itself. As noted above, the negative isostatic anomalies shown on Marussi's (1964) cross section over Indo–Gangetic Plains and the southern margin of the Tarim Basin probably can be explained by flexure of the Indian and Tarim plates to form foreland basins. The positive isostatic anomalies would be caused by the strength of the plates supporting the mountains and redistributing the buoyant response of their loads. Notice, however, that a negative isostatic anomaly characterizes the Karakoram Range (figure 21), implying that a mass deficit underlies the Karakoram. Marussi (1964) attributed this anomaly to a massive low-density granitic intrusion in the Karakoram, but I suspect that its source might be deeper.

We can estimate the mass deficit per unit length (δM) from the integral of the isostatic gravity anomaly (δg) over the horizontal distance

$$2\pi G \delta M = \int_{-\infty}^{\infty} \delta g(x)\, \mathrm{d}x,$$

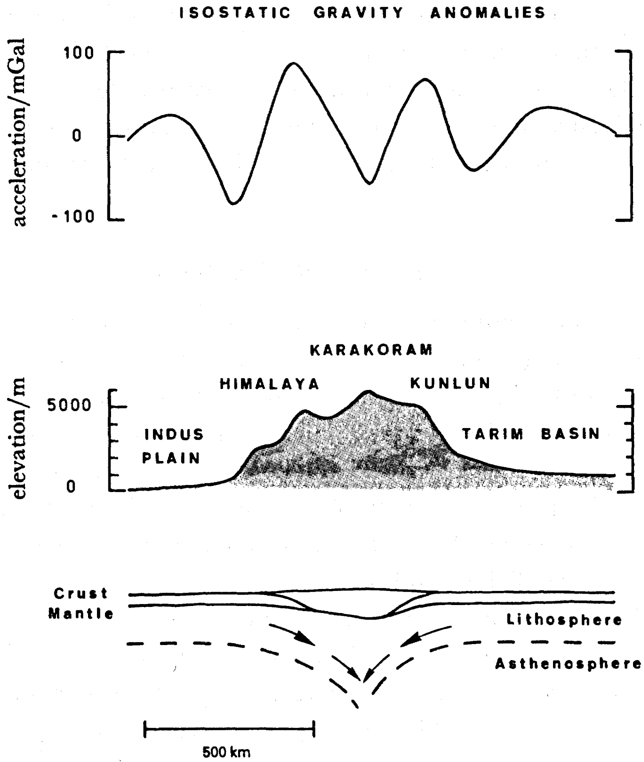

FIGURE 21. Sketches of isostatic anomalies, of topography and of a simple cross section across the Himalaya, the Karakoram and the Kunlun. Note the negative isostatic anomalies over the foreland basins of the Himalaya and the Kunlun, positive values over the Himalaya and the Kunlun, and negative anomalies over the Karakoram. I suspect that downwelling in the mantle holds the Karakoram out of isostatic equilibrium. (Gravity profile redrawn from Marussi 1964.)

where $2\pi G = 4.18 \times 10^{-5}$ mGal m^2 kg^{-1}. Ignoring other contributions to the gravity field, the minimum value of -60 mGal and the width of about 120 km for this anomaly would imply that the value of the integral is about 4×10^6 mGal m, corresponding to a mass deficit per unit length parallel to the chain of about 10^{11} kg m^{-1}. This mass deficit would contribute force per unit length of 10^{12} N m^{-1}, which is comparable in magnitude to the force applied to the end of the Indian Plate in the calculations of Lyon-Caen & Molnar (1983, 1985). Thus, neither the force nor the mass deficit is small.

The mass deficit per unit length, if caused by granite with a density 50 kg m^{-3} less than the surrounding rock would imply a large cross-sectional area of 2000 km^2. Were it caused by an unusually deep Moho, with a density contrast of 500 kg m^{-3}, it would be consistent with an average excess thickness of crust of 4 km over a width of 50 km.

The narrow width of isostatic anomaly might at first suggest that its source could not be as deep as 70–80 km, near the Moho; but the data defining it are neither abundant nor as accurate as modern data. Moreover, if the crust were unusually deep beneath the Karakoram, there must be a force holding it down, and stresses induced by the downwelling of cold material would be a likely force (figure 21). The mass excess associated with this cold material would contribute a positive anomaly. Thus the measured isostatic anomaly would be the difference between two larger anomalies: a negative one due to the overthickening (with respect to isostatic equilibrium) of the crust, and a positive one due to the cold, thickened downwelling root of mantle lithosphere. Thus, both the dimensions and the amplitude of this negative isostatic anomaly might give underestimates of the possible deflection of the Moho.

Clearly the explanation of Marussi's (1964) negative isostatic anomaly over the Karakoram in terms of a thickened crust drawn down by a cold mantle root is not unique. Moreover, the anomaly is not well enough defined to make quantitative analysis useful. Nevertheless, I think it worth considering.

Seismic studies of the Karakoram

The Karakoram is unusual by being underlain by a zone of intermediate depth earthquakes (Chen & Roecker 1981), and there is a hint that the shear wave velocity in the upper mantle is high (Brandon & Romanowicz 1986). Both suggest that the uppermost mantle is colder than normal.

Seismicity

Intermediate depth earthquakes (70 km $\leqslant$ depth $\leqslant$ 300 km) are very rare except where oceanic lithosphere has clearly been subducted since 10 Ma or so. Consequently, those few narrow and well-defined belts of intense seismic activity at intermediate depths in continental regions (Hindu Kush, Pamir, Romania and Burma) are usually ascribed to late-Cainozoic subduction of oceanic lithosphere, even where convincing geologic evidence for the suturing of continental fragments in late-Cainozoic time is absent. In addition, there are few areas of the earth where intermediate depth earthquakes have unequivocally occurred in the last 20 years, but where subduction of oceanic lithosphere since 20 Ma almost surely has not occurred (Chen & Molnar 1983; Chen *et al.* 1981; Hatzfeld & Frogneux 1981). Above, we noted two such earthquakes in southern Tibet. The Karakoram appears to be the intracontinental region with the most active diffuse intermediate depth seismicity, possibly with the largest of such earthquakes, and with many of the deepest (up to 100 km) (Chen & Molnar 1983; Chen & Roecker 1981). This zone does not appear to be a continuation of the seismic zone that dips southward beneath the Pamir and that may represent late-Tertiary subduction of oceanic lithosphere (see, for example, Billington *et al.* 1977; Roecker *et al.* 1980).

Estimates of temperatures of the material in which earthquakes in the mantle occur are virtually all less than 800 °C, and most are less than 600 °C (see, for example, Chen & Molnar 1983; Molnar *et al.* 1979). In so far as those estimates are reasonable, the occurrence of earthquakes at depths of 100 km beneath the Karakoram would imply very low average geothermal gradients of less than 8 K km^{-1}, and probably less than 6 K km^{-1}. Thus, the occurrence of these earthquakes implies a relatively cold upper mantle beneath the Karakoram.

Seismic-wave velocities

In addition to studying Rayleigh-wave phase velocities across Tibet (discussed above), Brandon & Romanowicz (1986) analysed paths across the Karakoram and Pamir. Although the structure along these paths is probably complex, and their main focus was not on this area, they could resolve unusually high phase velocities for paths across this area. In fitting measured and calculated phase velocities, they concluded that the shear wave velocity is approximately 5 km s^{-1} in the uppermost mantle. This is an extremely high velocity, probably too high to be explained solely by a low temperature of the material. This I suspect that the velocity is not tightly constrained. Nevertheless, the relatively high phase velocity seems to be required, and therefore, so is a relatively high shear-wave velocity in the mantle.

In addition, among the earthquakes in the Himalaya and Tibet for which Molnar & Chen (1984) measured S-wave residuals, the earthquake with the largest negative residual occurred in the western Himalaya just southwest of the Karakoram (figure 9). These relatively early arrivals are also consistent material with relatively high velocities underlying the northwestern Himalaya (and the Karakoram); one earthquake, however, constitutes only a suggestion and certainly not proof.

Summary of constraints on the deep structure of the Karakoram

Taken together, the existence of intermediate depth earthquakes, the high phase velocity of Rayleigh waves (Brandon & Romanowicz 1986), and one earthquake with relatively early S-waves suggest that the mantle beneath the Karakoram is unusually cold, and the gravity anomalies along a profile crossing the Karakoram can be interpreted in terms of cold material sinking beneath the range and drawing the Moho down (figure 21). This interpretation is certainly not unique, and the seismic data do not place a quantitative constraint on the degree to which the temperature in the mantle beneath the Karakoram is lower than that beneath a shield. What can be said is that the deep structure of the Karakoram is different both from that of most of Tibet (if not all of Tibet) and from that of the Himalaya, and that it is consistent with what one might expect of the uppermost mantle beneath a region of intense crustal shortening. As usual, there are enough data to suggest a plausible interpretation, but not to prove or to refine it.

Summary and synthesis

Like that of all regions, the deep structure of Tibet, the Himalaya and the Karakoram is a consequence of geologic processes operating for millions to tens of millions of years. Because we can know the deep structure at only a brief instant in geologic time, the knowledge of it for any region can rarely be used to decide uniquely which among a number of proposed tectonic evolutions of the region is correct. Nevertheless, given the rather limited knowledge of the geologic history of the Himalaya and especially that of Tibet and the Karakoram, the deep structure of these regions provides an important constraint on their possible tectonic evolutions. Moreover, because gravity acting differently on density variations within Earth is almost surely the principal driving force of large-scale tectonic processes, a knowledge of lateral variations in structure is fundamental for understanding dynamic processes in the earth. This review has focused on these two aspects of the deep structure: (1) as a constraint on suggested and plausible tectonic evolutions of the world's highest plateau and mountain chain and (2) as a clue to understanding the dynamic processes that have built these extraordinary features.

Virtually all proposed scenarios for the evolution and for the support of the Himalaya and Tibet include the presumption that the crustal thickness increases from a relatively normal value beneath India to a value of about 70 km beneath the plateau. Geophysical evidence of a variety of kinds supports this presumption, in a general form. Seismic refraction profiles across the stable parts of India reveal an average crustal thickness of about 38 km (Kaila 1982). Bouguer-gravity anomalies become increasingly negative from the Central India Highlands, across the Indo–Gangetic Plains and the Himalaya, to southern Tibet (Das *et al.* 1979; Kono

1974; Qureshy *et al.* 1974). The few published measurements from Tibet and its margins indicate large negative values and are consistent with a very thick crust (Amboldt 1948; Marussi 1964). Wide-angle reflections from the Moho indicate an increasing depth of the Moho from about 55 km beneath the Greater Himalaya, and apparently shallower farther south, to 70–75 km beneath the southern edge of Tibet (Hirn & Sapin 1984; Hirn *et al.* 1984*a*; Lépine *et al.* 1984). Clear wide-angle reflections from studies farther north, in the southern half of Tibet, indicate a depth of the Moho of about 70 km in some, but not all, areas (Hirn *et al.* 1984*b*, *c*). Hirn, Lépine, Sapin and their colleagues have inferred the existence of steps, instead of smooth variations, in the Moho beneath the Himalaya and beneath Tibet, but as noted above, I remain unconvinced of these steps. Finally, surface-wave dispersion across most of Tibet corroborates the existence of a thick crust over most of Tibet (Chen 1979; Chen & Molnar 1981; Jobert *et al.* 1985; Romanowicz 1982). Thus, to a good first approximation, it is reasonable to assume that Tibet is underlain by a thick crust.

The average crustal thickness of Tibet appears to be 65–70 km. It clearly is not as great as 80 km or as little as 55 km. Locally the thickness seems to reach 75 km, just north of the Greater Himalaya and south of the Indus–Tsangpo Suture Zone (Hirn & Sapin 1984). In north–central Tibet, in an area a few hundred kilometres in dimension, the thickness appears to be only 50–60 km (Brandon & Romanowicz 1986). Hirn *et al.* (1984*b*) recorded strong variations in the wide-angle reflections that they associate with lateral variations in crustal thickness of as much as 15–30 km over distances of tens of kilometres. The crustal thickness beneath the Greater Himalaya, where the highest elevations are found but also where the mean elevation is similar to that beneath southern Tibet (Bird 1978), is about 55 km (Hirn & Sapin 1984; Lépine *et al.* 1984), much smaller than that farther north. Thus, although to a good first approximation the crustal thickness of Tibet is double that of most areas and this large thickness compensates for the remarkably uniform, high elevation of the plateau, both marked lateral heterogeneity and large deviations from isostatic equilibrium must exist beneath the Himalaya and Tibet.

The recognition of marked lateral heterogeneity in the mantle beneath Tibet is one of the important discoveries of the structure of Tibet made in the 1980s and suggests that simple Airy-type isostatic compensation does not prevail over all of Tibet. The variations in surface-wave dispersion that indicate a relatively thin crust beneath north–central Tibet also imply that the shear wave velocity in the underlying uppermost mantle is much lower there than elsewhere beneath Tibet and the Himalaya (Brandon & Romanowicz 1986). Large delays of S-waves from earthquakes in north–central Tibet and recorded at teleseismic distances indicate that the mean shear-wave velocity in the uppermost mantle is 4–8% lower than that beneath the Himalaya (Molnar & Chen 1984; Pettersen & Doornbos 1987). Waveforms and travel times of shear waves recorded at regional distances (less than 30°) corroborate the inference that the material with the low shear-wave velocity is in the upper 250 km of the Earth and not deeper (Lyon-Caen 1986). Finally, the phase Sn, which propagates in the upper 100 km or so of the mantle, is attenuated on paths crossing north–central Tibet, suggesting very low Q in the uppermost mantle of this area (Ni & Barazangi 1983). Taken together, the low shear-wave velocities and the high attenuation in the mantle suggest that the mantle beneath north–central Tibet is unusually hot, an inference that accords with the existence of recent basic volcanism in this part of Tibet (Burke *et al.* 1974; Deng 1978; Kidd 1975; Molnar *et al.* 1987*a*).

Except for the volcanism, the topography of northern Tibet gives no hint of a relatively thin

PHILOSOPHICAL TRANSACTIONS OF THE ROYAL SOCIETY A MATHEMATICAL, PHYSICAL & ENGINEERING SCIENCES

crust or a relatively hot upper mantle. Thus I presume that the high, uniform elevation is isostatically compensated. (There are no published gravity measurements to test this.) Clearly the thinner crust suggests that if Airy isostasy prevails elsewhere in Tibet, it does not do so in north–central Tibet. Correspondingly the inference of high temperature in the uppermost mantle suggests that relatively light material in the mantle contributes to this compensation. Thus, in my view, the relatively uniform height of the Tibetan Plateau masks an important feature: the existence of relatively thin crust overlying relatively hot uppermost mantle beneath north–central Tibet.

The variation in crustal thickness implies that whatever the process is that built the Tibetan Plateau, it did not do so with the uniformity implied by the uniform elevation. If the Indian crust slid beneath Tibet, it probably has not slid beneath northern Tibet. If crustal shortening, within what was southern Eurasia before the collision, built the plateau, then the shortening has not been uniform across the plateau. In general, the existence of lateral variations in temperature in the mantle is both a prerequisite for and a direct manifestation of thermal convection. Thus I suspect that north–central Tibet is the locus of convective upwelling of hot material in the upper mantle (figure 22). The corresponding downwelling would lie astride the upwelling, probably beneath southern Tibet and perhaps also beneath northernmost Tibet.

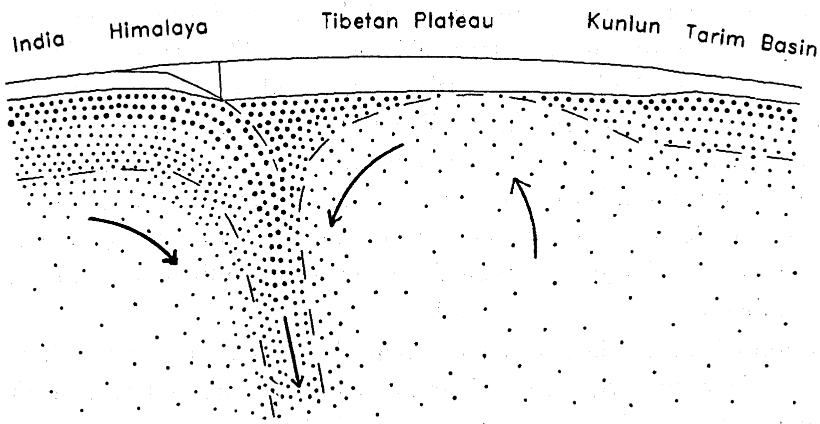

FIGURE 22. Idealized cross section across the Himalaya and Tibet illustrating differences in crustal thickness and origin, as well as hypothetical subduction of Indian mantle lithosphere and induced convective circulation in the asthenosphere.

The existence of cold material in the upper mantle is implied by the shield structures beneath India and beneath the Tarim Basin. Moreover, the evidence for active crustal shortening in the Himalaya and on the northern margin of Tibet (Molnar *et al.* 1987*a*, *b*) imply an active underthrusting of the shields beneath these margins of Tibet. Thus we might look to the transitions from these shield structures at the margins of Tibet to search for evidence of cold downwelling material in the mantle.

A study of shear waves crossing the Indian Shield confirms that it is underlain by a thick high-velocity layer with only a minor low-velocity zone beneath it (Lyon-Caen 1986). Several observations imply that this thick lithosphere has been thrust beneath the Himalaya, at least 80 km and probably more than 100 km. Fault-plane solutions and focal depths of many of the moderate earthquakes suggest that these events have occurred on the top surface of the intact Indian plate, some 80–100 km north of the front of the range (Baranowski *et al.* 1984; Ni &

Barazangi 1984). Gravity anomalies over the Indo–Gangetic Plain imply that the underlying Ganga Basin has formed by the flexure of the Indian plate, and those from the Lesser Himalaya imply that the plate extends 100 km beneath this part of the range, with the Moho dipping at the same gentle angle (*ca.* 3–5°) as beneath the Ganga Basin (Lyon-Caen & Molnar 1983, 1985). Travel times of P-waves recorded at the Tarbella array, which spans the Lesser Himalaya in part of Pakistan, also imply a gentle dip of about 4° of the Moho (Menke 1977). Finally, arrival times of S-waves from earthquakes in the Himalaya are consistent with that area being underlain by a shield-like upper mantle (Molnar & Chen 1984).

The structure of the mantle beneath the Greater Himalaya and southernmost Tibet is less unequivocally defined. There is little doubt that crustal thickness increases from south to north. Whereas Hirn & Sapin (1984) and Lépine *et al.* (1984) inferred that this increase is manifested by steps in the Moho at southward-dipping thrusts faults, I think that some of their data, at least, can be interpreted in terms of a smooth increase in the depth of a northward dipping Moho. In either case, gravity anomalies imply that the average dip of the Moho is steeper beneath the Greater Himalaya ($\delta \approx 15°$) than beneath the Lesser Himalaya ($\delta \approx 3$–$5°$) (Kono 1974; Lyon-Caen & Molnar 1983, 1985; Warsi & Molnar 1977). If the Indian plate extends beneath the Greater Himalaya, this increase in dip requires that the plate be bent more sharply than it is beneath the Lesser Himalaya. The bending of the plate seems to be the result of dynamic forces acting on the mantle lithosphere north of the Greater Himalaya (Lyon-Caen & Molnar 1983, 1985).

The upper-mantle structure of southern Tibet near the Indus–Tsangpo Suture Zone is uncertain because of limited data and conflicting interpretations. There is a suggestion of a very high Pn velocity (8.5–8.7 km s^{-1}), which might indicate a deep high-velocity layer (Hirn & Sapin 1984; Menke & Jacob 1976). The occurrence of two earthquakes at depths of 90 km beneath southern Tibet suggests the existence of relatively low temperatures there (Chen *et al.* 1981; Molnar & Chen 1983). It is my prejudice that mantle beneath southernmost Tibet is relatively cold (figure 22), but neither of these observations are strong evidence for this prejudice. Moreover, it conflicts with the inference from long-period surface-wave dispersion that the high-velocity layer in the uppermost mantle is thin and extends to a depth of only 100 km or so (Jobert *et al.* 1985).

The southern margin of the low-velocity region of north–central Tibet is also poorly defined. The phases Pn and Sn propagate efficiently and with high velocities through the uppermost mantle of central, southern, eastern and western Tibet (Ni & Barazangi 1983). Delays of S-waves, both to distant stations (more than 30°) (Molnar & Chen 1984; Pettersen & Doornbos 1987) and to regional distances (less than 30°) from the few earthquakes studied in central and southern Tibet (Lyon-Caen 1986), suggest that the average upper-mantle velocity beneath central and southern Tibet is lower than that beneath the Himalaya and higher than that beneath north–central Tibet. Although these observations could be taken as evidence that the thickness of the high-velocity layer in the uppermost mantle increases southward from central to southern Tibet (figure 22), the sparsity of observations does not require this to be so.

The lateral variations in the mantle beneath Tibet are too poorly resolved to allow a quantitative, or even qualitatively definitive, constraint on the processes that built Tibet. The S-wave travel times, in particular, indicate that the structure beneath most of Tibet (more than half and probably at least two thirds) is not that of a shield. Therefore, if the Indian Shield did underthrust most or all of Tibet, the mantle portion of that lithosphere has been modified

PHILOSOPHICAL TRANSACTIONS OF THE ROYAL SOCIETY A MATHEMATICAL, PHYSICAL & ENGINEERING SCIENCES

substantially since that underthrusting occurred. Neither the absence of a shield-like upper-mantle structure, nor any of the arguments that follow prove that India has not underthrust all of Tibet, but obviously they require that proponents of that view explain where their shield has gone.

The present deep structure of Tibet and the Himalaya are consistent with the Indian Shield underthrusting only the southernmost 100–300 km of Tibet and with the thick crust being a consequence of crustal shortening within the ancient southern margin of Eurasia (Dewey & Burke 1973; England & Houseman 1986). When crustal shortening and crustal thickening occur, the underlying mantle lithosphere initially attached to the crust, must also undergo horizontal shortening and thickening. The thickening of the mantle lithosphere advects cold isotherms downwards, and therefore produces horizontal temperature gradients. The advection of this cold material, therefore, is likely to induce thermal convection in the asthenosphere that will draw the lower part of the neighbouring lithosphere into the downgoing limb of the cell (Fleitout & Froidevaux 1982; Houseman *et al.* 1981). This material will be replaced by hotter material from below. England & Houseman (1988) infer that recent uplift of Tibet is caused by such a replacement of the cold, thickened lithospheric root by such material. My image of the mantle dynamics beneath Tibet includes downwelling beneath southern Tibet, upwelling beneath north–central Tibet, and possibly downwelling also beneath the northern margin of Tibet (figure 22).

The downwelling on the southern margin of Tibet should be enhanced by the continued underthrusting of the Indian Shield beneath the Himalaya. As noted above, both gravity anomalies over the Lesser Himalaya and wide-angle reflection profiles over the Greater Himalaya indicate that the crustal thickness beneath the Himalaya is much smaller than it would be if local Airy-type isostatic equilibrium prevailed. The flexure of a strong Indian plate helps to support the high range of mountains, but numerical experiments with plates of various flexural rigidities show that the strength of the plate cannot by itself support the range; an additional force is necessary (Lyon-Caen & Molnar 1983, 1985). A bending moment applied to underthrust the India plate, or perhaps some other dynamic process, could flex the plate beneath the Lesser Himalaya up a few kilometres to shallower depths than it would be if it were depressed solely by the weight of the Himalaya. The moment could be produced by the downward force of gravity acting on the cold slab of India's mantle lithosphere from which all or much of the crust has been detached at the Himalaya (figure 22). The plunging of this mantle lithosphere, in turn, would help to draw the lower part of southern Tibet's mantle lithosphere into the asthenosphere.

This interpretation of the mantle dynamics beneath the Himalaya and Tibet is by no means proven and is surely an oversimplification. The only evidence even suggestive of subduction of Indian mantle lithosphere beneath southern Tibet is the indirect evidence from gravity anomalies interpreted in terms of a flexed plate acted upon by an additional force to support the Himalaya.

If both of these processes have occurred in Asia (shortening of Tibet's underlying mantle lithosphere and underthrusting of India's mantle lithosphere beneath southern Tibet), the area where manifestations of these processes are likely to be clearest is near the Karakoram. In that area, both northward underthrusting of the India Shield beneath the Himalaya and southward underthrusting of the Tarim Basin shield beneath the Kunlun (Lyon-Caen & Molnar 1984; Norin 1946) seem to continue. This is the area where diffusely distributed intermediate depth seismicity is most prevalent on Earth (Chen & Roecker 1981), suggesting both rapid deformation and low temperatures in the upper mantle. Moreover, shear-wave velocities in the upper 100 km of the mantle appear to be unusually high (Brandon & Romanowicz 1986), also suggesting low temperatures there. Thus, what little evidence exists is consistent with the presence of a root to the bottom of the mantle lithosphere, if not active downwelling.

The hypothesized dynamics of the mantle described above do not constitute original ideas; variations of them have been proposed before both as general processes (Fleitout & Froidevaux 1982; Houseman *et al.* 1981) and specifically for the Alps (Panza & Mueller 1979), the Apennines (Royden & Karner 1984), the Pyrenees (Brunet 1986) and the transverse ranges of California (Humphreys *et al.* 1984; Sheffels & McNutt 1986). In these areas where the geologic histories and geologic structures are relatively well known, the geophysical signatures of the structure of the mantle, however, appear to be more subtle than in the Himalaya, the Karakoram or Tibet, where the geologic history is still only crudely known. Thus, because only cruder methods than can be applied to these other areas, nevertheless, reveal large lateral variations in the deep structure of Asia, it is likely that with newer techniques, the resolution of such inhomogeneities beneath the Himalaya, the Karakoram, and Tibet will enhance our understanding of the dynamics of mountain building more than the refinement of the deep structure of more minor mountain belts. Thus continued scientific pilgrimages to the birthplace of geophysics as a geological or tectonic tool and the furtherance of a tradition established by Airy, Everest and Pratt more than 100 years ago are likely to provide a key to the understanding of the dynamics of mountain building.

I thank M. Barazangi, H. Lyon-Caen, and B. Romanowicz for providing me with figures from their published papers, and Dan McKenzie, F.R.S., for critically reading the manuscript. This research was supported in part by the Centre National de Recherches Scientifiques of France, by the National Science Foundation under grant 8500810-EAR and by the National Aeronautical and Space Administration under grant NAG4-795.

References

Acharya, S. K. & Ray, K. K. 1982 *Bull. Am. Ass. Petrol. Geol.* **66**, 57–70.

Airy, G. B. 1855 *Phil. Trans. R. Soc. Lond.* **145**, 101–104.

Allègre, C. J. *et al.* 1984 *Nature, Lond.* **307**, 17–22.

Amboldt, N. 1948 *Reports from Scientific Expedition to Northwestern Provinces of China under the Leadership of Dr. Sven Hedin, Publ. 30, Geodes.* Stockholm: Tryckeri Aktiebolaget Thule. (112 pages.)

Anderson, O. L., Schreiber, E., Liebermann, R. C. & Soga, N. 1968 *Rev. Geophys.* **6**, 491–524.

Argand, E. 1924 *Int. Geol. Cong. Rep. Sess.* **13** (1), 170–372.

Baranowski, J., Armbruster, J., Seeber, L. & Molnar, P. 1984 *J. geophys. Res.* **89**, 6918–6928.

Barazangi, M. & Ni, J. 1982 *Geology* **10**, 179–185.

Beloussov, V. V., Belyaevsky, N. A., Borisov, A. A., Volvovsky, B. S., Volkovsky, I. S., Resvoy, D. P., Tal-Virsky, B. B., Khamrabaev, I. Kh., Kaila, K. L., Narain, H., Marussi, A. & Finetti, J. 1980 *Tectonophysics* **70**, 193–221.

Billington, S., Isacks, B. L. & Barazangi, M. 1977 *Geology* **5**, 699–704.

Bird, G. P. 1976 Ph.D. thesis, Massachusetts Institute of Technology, U.S.A.

Bird, P. 1978 *J. geophys. Res.* **83**, 4975–4987.

Black, P. R. & Braile, L. W. 1982 *J. geophys. Res.* **87**, 10557–10568.

Brandon, C. & Romanowicz, B. 1986 *J. geophys. Res.* **91**, 6547–6564.

Brunet, M. F. 1986 *Tectonophysics* **129**, 343–354.

Burke, K. C. A., Dewey, J. F. & Kidd, W. S. F. 1974 *Geol. Soc. Am. Abstr. Programs* **6**, 1027–1028.

Cauët, R., Serryn, P. & Vincent, M. 1957 *Petit Atlas Bordas: la France, le Monde.* Paris: SCIP.

Chen, W.-P. 1979 Ph.D. thesis, Massachusetts Institute of Technology, U.S.A.

Chen, W.-P. & Molnar, P. 1981 *J. geophys. Res.* **85**, 5937–5962.
Chen, W.-P. & Molnar, P. 1983 *J. geophys. Res.* **88**, 4183–4214.
Chen, W.-P., Nabelek, J. L., Fitch, T. J. & Molnar, P. 1981 *J. geophys. Res.* **86**, 2863–2876.
Chen, W.-P. & Roecker, S. W. 1981 *Eos, Wash.* **61**, 1031.
Choudhury, S. K. 1975 *Geophys. Jl R. astr. Soc.* **40**, 441–452.
Chun, K.-Y. & McEvilly, T. V. 1986 *J. geophys. Res.* **91**, 10405–10411.
Chun, K.-Y. & Yoshii, T. 1977 *Bull. seism. Soc. Am.* **67**, 737–750.
Curray, J. R., & Moore, D. G. 1974 In *The geology of continental margins* (ed. C. A. Burk & C. L. Drake), pp. 617–628, New York: Springer-Verlag.
Das, D., Mehra, G., Rao, K. G. C., Roy, A. L. & Naraya, M. S. 1979 *Himalayan Geology Seminar, Section III, Oil and Natural Gas Resources, Geol. Surv. India*, misc. publ. **41**, 141–148.
Deng Wanming 1978 *Acta geol. sin.* **2**, 148–162.
Dewey, J. F. & Burke, K. C. A. 1973 *J. Geol.* **81**, 683–692.
Doyle, H. A. & Hales, A. L. 1967 *Bull. seism. Soc. Am.* **57**, 761–771.
Duroy, Y., Farah, A., Malinconico, L. L. & Lillie, R. J. 1988 In *Tectonics and geophysics of the Western Himalaya* (ed. L. L. Malinconico & R. J. Lillie). Geol. Soc. Amer. Spec. Pap. (In the press.)
England, P. C. & Houseman, G. A. 1986 *J. geophys. Res.* **91**, 3664–3676.
England, P. C. & Houseman, G. A. 1988 *J. geophys. Res.* (In the press.)
Ewing, M. & Press, F. 1959 *Bull. geol. Soc. Am.* **70**, 229–244.
Feng, C.-C. 1982 Ph.D. thesis, University of Southern California, Los Angeles.
Feng, C.-C. & Teng, T.-L. 1983 *J. geophys. Res.* **88**, 2261–2272.
Fleitout, L. & Froidevaux, C. 1982 *Tectonics* **1**, 21–56.
Francheteau, J., Jaupart, C., Shen Xianjie, Kang Wenhua, Lee Defu, Bai Jiachi, Wei Hungpin & Deng Hsiayeu 1984 *Nature, Lond.* **307**, 32–36.
Grand, S. & Helmberger, D. V. 1984 *Geophys. Jl R. astr. Soc.* **76**, 399–438.
Gupta, H. K. & Narain, H. 1967 *Bull. seism. Soc. Am.* **57**, 235–248.
Hatzfeld, D. & Frogneux, M. 1981 *Nature, Lond.* **292**, 443–445.
Herrin, E. 1968 *Bull. seism. Soc. Am.* **58**, 1193–1241.
Hirn, A. *et al.* 1984*a* *Nature, Lond.* **307**, 23–25.
Hirn, A., Jobert, G., Wittlinger, G., Xu Zhongxin & Gao Enyuan 1984*c* *Ann. Geophsicae* **2**, 113–117.
Hirn, A., Nercessian, A., Sapin, M., Jobert, G., Xu Zhongxin, Gao Enyuan, Lu Deyuan & Teng Jiwen 1984*b* *Nature, Lond.* **307**, 25–27.
Hirn, A. & Sapin, M. 1984 *Ann. Geophysicae* **2**, 123–130.
Houseman, G. A., McKenzie, D. P. & Molnar, P. 1981 *J. geophys. Res.* **86**, 6115–6132.
Huestis, S., Molnar, P. & Oliver, J. 1973 *Bull. seism. Soc. Am.* **63**, 469–475.
Humphreys, E., Clayton, R. W. & Hager, B. H. 1984 *Geophys. Res. Lett.* **11**, 625–627.
Institute of Geophysics, Academy of Sciences 1981 *Acta geophys. Sin.* **24**, 155–170.
Jaupart, C., Francheteau, J. & Shen Xian-jie 1985 *Geophys. Jl R. astro. Soc.* **81**, 131–155.
Jeffreys, H. & Bullen, K. E. 1940 *Seismological tables*. British Association Gray–Milne Trust.
Jia Su-juan, Cao Xue-feng & Yan Jia-quan 1981 *N West. seism. J.* **3**, 27–34.
Jobert, N., Journet, B., Jobert, G., Hirn, A. & Zhong, S. K. 1985 *Nature, Lond.* **313**, 386–388.
Johnson, B. D., Powell, C. M. & Veevers, J. J. 1976 *Bull. geol. Soc. Am.* **87**, 1560–1566.
Kaila, K. L. 1982 *Bull. geophys. Res.* **20**, 309–328.
Kaila, K. L., Krishna, V. G., Choudhury, K. & Narain, H. 1978 *J. geol. Soc. India* **19**, 1–20.
Karner, G. D. & Watts, A. B. 1983 *J. geophys. Res.* **88**, 10449–10477.
Karunakaran, C. & Ranga Rao, A. 1979 *Contributions to Stratigraphy and Structure, Himalayan Geology Seminar, Section III, Oil and Natural Gas Resources, Geol. Surv. India*, misc. publ. no. 41, pp. 1–66.
Kidd, W. S. F. 1975 *Eos, Wash.* **56**, 453.
Klootwijk, C. T., Conaghan, P. J. & Powell, C. M. 1985 *Earth planet. Sci. Lett.* **75**, 167–183.
Kono, M. 1974 *Geophys. Jl R. astr. Soc.* **39**, 283–300.
Lépine, J.-C., Hirn, A., Pandey, M. R. & Tater, J. M. 1984 *Ann. Geophysicae* **2**, 119–121.
Lillie, R. J. & Yousuf, M. 1986 In *Reflection seismology: the continental crust*. Am. Geophys. Un., Geodynamic Ser., vol. 14 (ed. M. Barazangi & L. Brown), pp. 55–65.
Lin Jian & Parmentier, E. M. 1985 *Geophys. Res. Lett.* **12**, 357–360.
Lyon-Caen, H. 1986 *Geophys. Jl R. astr. Soc.* **86**, 727–749.
Lyon-Caen, H. & Molnar, P. 1983 *J. geophys. Res.* **88**, 8171–8191.
Lyon-Caen, H. & Molnar, P. 1984 *Geophys. Res. Lett.* **11**, 1251–1254.
Lyon-Caen, H. & Molnar, P. 1985 *Tectonics* **4**, 513–538.
Marussi, A. 1964 *Geophysics of the Karakorum, Italian Expeditions to the Karakorum (K^2) and Hindu Kush, Sci. Rept. 2, 1.* (242 pages.)
McKenzie, D. P. 1967 *J. geophys. Res.* **72**, 6261–6273.
McKenzie, D. 1977 *Geophys. Jl R. astr. Soc.* **48**, 211–238.
McKenzie, D. P., Roberts, J. M. & Weiss, N. O. 1974 *J. Fluid Mech.* **62**, 465–538.

Menke, W. H. 1977 *Bull. seism. Soc. Am.* **67**, 725–734.
Menke, W. H. & Jacob, K. H. 1976 *Bull. seism. Soc. Am.* **66**, 1695–1711.
Mishra, D. C. 1982 *Earth planet. Sci. Lett.* **57**, 415–420.
Molnar, P. 1984 *A. Rev. Earth planet. Sci.* **12**, 489–518.
Molnar, P. 1988 *Ann. Geophys.* (In the press.)
Molnar, P., Burchfiel, B. C., Liang K'uangyi & Zhao Ziyun 1987*b* *Geology* **15**, 249–253.
Molnar, P., Burchfiel, B. C., Zhao Ziyun, Liang K'uangyi, Wang Shuji & Huang Minmin 1987*a* *Science, Wash.* **235**, 299–305.
Molnar, P. & Chen, W.-P. 1982 In *Mountain building processes* (ed. K. Hsü). London: Academic Press.
Molnar, P. & Chen, W.-P 1983 *J. geophys. Res.* **88**, 1180–1196.
Molnar, P. & Chen, W.-P. 1984 *J. geophys. Res.* **89**, 6911–6917.
Molnar, P., Freedman, D. & Shih, J. S. F. 1979 *Geophys. Jl R. astr. Soc.* **56**, 41–54.
Molnar, P. & Oliver, J. 1969 *J. geophys. Res.* **74**, 2648–2682.
Molnar, P. & Tapponnier, P. 1978 *J. geophys. Res.* **83**, 5361–5375.
Ni, J. & Barazangi, M. 1983 *Geophys Jl R. astr. Soc.* **72**, 665–689.
Ni, J. & Barazangi, M. 1984 *J. geopys. Res.* **89**, 1147–1163.
Norin, E. 1946 *Reports from the Scientific Expedition to the Northwestern Provinces of China under the Leadership of Dr. Sven Hedin, Publ. 29, (III), Geology 7*. Stockholm: Tryckeri Aktiebolaget Thule. (214 pages.)
Pandey, M. R. 1981 *J. Nepal geol. Soc.* **1**, 29–35.
Pandey, M. R. 1986 *J. Nepal geol. Soc.* **6**, 1–11.
Panza, G. F. & Mueller, S. 1979 *Mem. Sci. Geol.* **33**, 43–50.
Parsons, B. & Daly, S. 1983 *J. geophys. Res.* **88**, 1129–1144.
Patton, H. 1980*a* *J. geophys. Res.* **85**, 821–848.
Patton, H. 1980*b* *Rev. Geophys. Space Phys.* **18**, 605–625.
Pettersen, Ú. & Doornbos, D. J. 1987 *Phys. Earth planet. Int.* **47**, 125–136.
Pham, V. N., Boyer, D., Therme, P., Xue Cheng-yuan, Li Li & Guo Yuan-jin, 1986 *Nature, Lond.* **319**, 310–314.
Pines, I., Teng, T., Rosenthal, R. & Alexander, S. 1980 *J. geophys. Res.* **85**, 3829–3844.
Powell, C. M. & Conaghan, P. J. 1973 *Earth planet. Sci. Lett.* **20**, 1–12.
Powell, C. M. & Conaghan, P. J. 1975 *Geology* **3**, 727–731.
Pratt, J. H. 1855 *Phil. Trans. R. Soc. Lond.* **145**, 53–100.
Qureshy, M. N. 1969 *Tectonophysics* **7**, 137–157.
Qureshy, M. N. & Warsi, W. E. K. 1980 *Geophys. Jl R. astr. Soc.* **61**, 235–242.
Qureshy, M. N., Venkatachalam, S. V. & Subrahmanyam, C. 1974 *Bull. geol. Soc. Am.* **85**, 921–926.
Raiverman, V., Kunte, S. V. & Mukherjee, A. 1983 *Petrol. Asia J.* **6**, 67–92.
Richardson, S. W. & England, P. C. 1979 *Earth planet. Sci. Lett.* **42**, 183–190.
Roecker, S. W., Soboleva, O. V., Nersesov, I. L., Lukk, A. A., Hatzfeld, D., Chatelain, J.-L. & Molnar, P. 1980 *J. geophys. Res.* **85**, 1358–1364.
Romanowicz. B. 1982 *J. geophys. Res.* **87**, 6865–6883.
Royden, L. & Karner, G. D. 1984 *Nature, Lond.* **309**, 142–144.
Sapin, M., Wang Xiangjing, Hirn, A. & Xu Zhongxin 1985 *Ann. Geophysicae* **3**, 637–646.
Sastri, V. V, Bhandari, L. L., Raju, A. T. R. & Datta, A. K. 1971 *J. geol. Soc. India* **12**, 223–233.
Schreiber, E. & Anderson, O. L. 1967*a* *J. geophys. Res.* **72**, 762–764.
Schreiber, E. & Anderson, O. L. 1967*b* *J. geophys. Res.* **72**, 3751.
Seeber, L. & Armbruster, J. 1981 In *Earthquake Prediction: An International Review, Maurice Ewing Series 4* (ed. D. W. Simpson & P. G. Richards), pp. 259–277. Washington, D.C.: Am. Geophys. Un.
Seeber, L., Armbruster, J. & Quittmeyer, R. 1981 In *Zagros, Hindu-Kush, Himalaya, Geodynamic Evolution, Geodyn. Ser.*, vol. 3, pp. 215–242. Washington, D.C.: Am. Geophys. Un.
Sengör, A. M. C. & Kidd, W. S. F. 1979 *Tectonphysics* **55**, 361–376.
Sheffels, B. & McNutt, M. 1986 *J. geophys. Res.* **91**, 6419–6431.
Sipkin, S. A. & Jordan, T. H. 1975 *J. geophys. Res.* **80**, 1474–1484.
Sipkin, S. A. & Jordan, T. H. 1980 *J. geophys. Res.* **85**, 853–861.
Smithson, S. B., Brewer, J. A., Kaufman, S., Oliver, J. E. & Hurich, C. A. 1979 *J. geophys. Res.* **84**, 5955–5972.
Soga, N., Schreiber, E. & Anderson, O. L. 1966 *J. geophys. Res.* **71**, 5315–5320.
Tang Bo-xiong, Liu Yuan-long, Zhang Li-min, Zhou Wen-hu & Wang Qian-shen 1981 In *Geological and ecological studies of Qinghai–Xizang Plateau*, pp. 683–689. Beijing: Science Press.
Teng Ji-wen 1981 In *Geological and ecological studies of Qinghai–Xizang Plateau*, pp. 633–649. Beijing: Science Press.
Teng Ji-wen *et al.* 1981 In *Geological and ecological studies of Qinghai–Xizang Plateau*, pp. 691–709. Beijing: Science Press.
Teng Ji-wen, Sun Ke-zhong, Xiong Shao-bai, Yin Zhou-xun, Yao Hung & Chen Li-fang 1983 *Phys. Earth planet. Int.* **31**, 293–306.
Teng J., Wang S., Yao Z., Xu Z., Zhu Z., Yang B. & Zhou W. 1980 *Acta Geophys. Sin.* **23**, 254–268.

Teng Ji-wen, Xiong Shao-bai, Yin Zhou-xun, Xu Zhong-xin, Wang Xiang-jing & Lu De-yuan 1985 *J. Phys. Earth* **33**, 157–171.
Tung, J. P. & Teng, T. L. 1974 *Eos, Wash.* **55**, 359.
Turcotte, D. L. & Schubert, G. 1982 *Geodynamics: applications of continuum mechanics to geological problems*, pp. 104–133. New York: John Wiley and Sons.
Wang, Chi-yuen, Shi, Y. & Zhou, W. 1982 *J. geophys. Res.* **87**, 2949–2957.
Warsi, W. E. K. & Molnar, P. 1977 In *Himalaya: sciences de la terre* (Colloques Internationaux du CNRS, no. 268), pp. 463–478. Paris: Editions du Centre National de la Recherche Scientifique.
Zhao, W.-L. & Morgan, W. J. 1985 *Tectonics* **4**, 359–369.
Zhou Wen-hu, Yang Zhan-shou, Zhu Hong-bin & Wu Li-gao 1981 In *Geological and ecological studies of Qinghai–Xizang Plateau*, pp. 673–682. Beijing: Science Press.

MATHEMATICAL, PHYSICAL & ENGINEERING SCIENCES
THE ROYAL SOCIETY
PHILOSOPHICAL TRANSACTIONS OF